



Virginia Center *for* Transportation
**INNOVATION
& RESEARCH**

Investigation of Panel-to-Panel Connections and Block-outs for Full-Depth Precast Concrete Bridge Decks

http://www.virginiadot.org/vtrc/main/online_reports/pdf/15-r5.pdf

MATTHEW K. SWENTY, Ph.D.
Assistant Professor
Virginia Military Institute

THOMAS E. COUSINS, Ph.D., P.E.
Professor
Via Department of Civil and Environmental Engineering
Virginia Polytechnic Institute and State University

CARIN L. ROBERTS-WOLLMANN, Ph.D., P.E.
Professor
Via Department of Civil and Environmental Engineering
Virginia Polytechnic Institute and State University

Final Report VCTIR 15-R5

Standard Title Page - Report on Federally Funded Project

1. Report No. FHWA/VCTIR 15-R5	2. Government Accession No.	3. Recipient's Catalog No.	
4. Title: Investigation of Panel-to-Panel Connections and Block-outs for Full-Depth Precast Concrete Bridge Decks		5. Report Date June 2015	
		6. Performing Organization Code	
7. Author(s) Matthew K. Swenty, Thomas E. Cousins, Ph.D., P.E., and Carin L. Roberts-Wollmann, Ph.D., P.E.		8. Performing Organization Report No. VCTIR 15-R5	
9. Performing Organization and Address Virginia Center for Transportation Innovation and Research 530 Edgemont Road Charlottesville, VA 22903		10. Work Unit No. (TRAIS)	
		11. Contract or Grant No. 82670	
12. Sponsoring Agencies' Name and Address Virginia Department of Transportation Federal Highway Administration 1401 E. Broad Street 400 North 8th Street, Room 750 Richmond, VA 23219 Richmond, VA 23219-4825		13. Type of Report and Period Covered Final Contract	
		14. Sponsoring Agency Code	
15. Supplementary Notes			
16. Abstract <p>Experimental tests were performed at Virginia Tech to investigate transverse panel-to-panel connections and horizontal shear connector block-outs for full-depth precast concrete bridge deck panels. The connections were designed for a deck replacement project for a rural three-span continuous steel beam bridge in Virginia. Two reinforced and four post-tensioned connections were designed and tested in cyclical loading. Each connection was tested on a full-scale, two-beam setup in negative bending with a simulated HS-20 vehicle. The block-outs for the horizontal shear connections were also scrutinized during construction and testing. Several surface treatments were investigated to determine the best strategy to limit cracking and leakage at the grout-concrete interface. The strain profile, cracking patterns, and ponding results are presented for all specimens.</p> <p>The reinforced connections and two post-tensioned connections with 167 psi initial stress experienced cracking and leaked water by the end of the cyclic loading regime. In two connections post-tensioned with an initial compressive stress of 340 psi, the tensile stress in the deck under full live load remained below approximately $3\sqrt{f_c}$. These transverse connections did not leak water, did not have full-depth cracking, and maintained a nearly linear strain distribution throughout the design life. Full-depth deck panels may be effectively used on continuous bridges if post-tensioning force is applied to the transverse connections to keep the total tensile stress (remaining prestress minus live load stress) below $3\sqrt{f_c}$.</p> <p>The block-outs with a sand-blasted surface or an epoxy primer combined with a grout that met the requirements recommended by Scholz et al. (2007) had only slight water leakage, and had smaller cracks at the grout-concrete interface than the control samples. These surface treatments are recommended for best long-term performance.</p>			
17 Key Words Full-depth precast bridge deck panels, Panel-to-panel connections, block-out surface treatments		18. Distribution Statement No restrictions. This document is available to the public through NTIS, Springfield, VA 22161.	
19. Security Classif. (of this report) Unclassified	20. Security Classif. (of this page) Unclassified	21. No. of Pages 71	22. Price

FINAL REPORT

**INVESTIGATION OF PANEL-TO-PANEL CONNECTIONS AND BLOCK-OUTS
FOR FULL-DEPTH PRECAST CONCRETE BRIDGE DECKS**

Matthew K. Swenty, Ph.D.
Assistant Professor
Virginia Military Institute

Thomas E. Cousins, Ph.D., P.E.
Professor
Via Department of Civil and Environmental Engineering
Virginia Polytechnic Institute and State University

Carin L. Roberts-Wollmann, Ph.D., P.E.
Professor
Via Department of Civil and Environmental Engineering
Virginia Polytechnic Institute and State University

Project Manager
Michael C. Brown, Ph.D., P.E.
Virginia Center for Transportation Innovation and Research

In Cooperation with the U.S. Department of Transportation
Federal Highway Administration

Virginia Center for Transportation Innovation and Research
(A partnership of the Virginia Department of Transportation
and the University of Virginia since 1948)

Charlottesville, Virginia

June 2015
VCTIR 15-R5

DISCLAIMER

The project that is the subject of this report was done under contract for the Virginia Department of Transportation, Virginia Center for Transportation Innovation and Research. The contents of this report reflect the views of the author(s), who is responsible for the facts and the accuracy of the data presented herein. The contents do not necessarily reflect the official views or policies of the Virginia Department of Transportation, the Commonwealth Transportation Board, or the Federal Highway Administration. This report does not constitute a standard, specification, or regulation. Any inclusion of manufacturer names, trade names, or trademarks is for identification purposes only and is not to be considered an endorsement.

Each contract report is peer reviewed and accepted for publication by staff of Virginia Center for Transportation Innovation and Research with expertise in related technical areas. Final editing and proofreading of the report are performed by the contractor.

Copyright 2015 by the Commonwealth of Virginia.
All rights reserved.

ABSTRACT

Experimental tests were performed at Virginia Tech to investigate transverse panel-to-panel connections and horizontal shear connector block-outs for full-depth precast concrete bridge deck panels. The connections were designed for a deck replacement project for a rural three-span continuous steel beam bridge in Virginia. Two reinforced and four post-tensioned connections were designed and tested in cyclical loading. Each connection was tested on a full-scale, two-beam setup in negative bending with a simulated HS-20 vehicle. The block-outs for the horizontal shear connections were also scrutinized during construction and testing. Several surface treatments were investigated to determine the best strategy to limit cracking and leakage at the grout-concrete interface. The strain profile, cracking patterns, and ponding results are presented for all specimens.

The reinforced connections and two post-tensioned connections with 167 psi initial stress experienced cracking and leaked water by the end of the cyclic loading regime. In two connections post-tensioned with an initial compressive stress of 340 psi, the tensile stress in the deck under full live load remained below approximately $3\sqrt{f'_c}$. These transverse connections did not leak water, did not have full-depth cracking, and maintained a nearly linear strain distribution throughout the design life. Full-depth deck panels may be effectively used on continuous bridges if post-tensioning force is applied to the transverse connections to keep the total tensile stress (remaining prestress minus live load stress) below $3\sqrt{f'_c}$.

The block-outs with a sand-blasted surface or an epoxy primer combined with a grout that met the requirements recommended by Scholz et al. (2007) had only slight water leakage, and had smaller cracks at the grout-concrete interface than the control samples. These surface treatments are recommended for best long-term performance.

FINAL REPORT

INVESTIGATION OF PANEL-TO-PANEL CONNECTIONS AND BLOCK-OUTS FOR FULL-DEPTH PRECAST CONCRETE BRIDGE DECKS

Matthew K. Swenty, Ph.D.
Assistant Professor
Virginia Military Institute

Thomas E. Cousins, Ph.D., P.E.
Professor
Via Department of Civil and Environmental Engineering
Virginia Polytechnic Institute and State University

Carin L. Roberts-Wollmann, Ph.D., P.E.
Professor
Via Department of Civil and Environmental Engineering
Virginia Polytechnic Institute and State University

INTRODUCTION

Each year, the average person spends almost a week waiting in traffic (Longman, 2001). Reports have suggested traffic delays cost the United States billions of dollars (Holguin, 2005). A number of issues contribute to traffic congestion, but one of the most prominent is construction delays. Construction is a necessary process that transportation officials must manage efficiently to maintain, rehabilitate, and build highways. Improving the materials and methods for constructing and rehabilitating bridges can reduce disruption to the traveling public.

One of the largest and longest processes in bridge construction is building the deck. Bridge deck construction is labor intensive, places workers in dangerous situations in staged construction, and costs a significant amount of money. Traditionally, bridge decks have been built of cast-in-place concrete. This type of construction requires extensive work forming the deck, placing the reinforcing steel, placing the concrete, and waiting for the concrete to cure. If a method could be devised to eliminate or speed up these processes, construction delays could be reduced and bridges with deck replacements would reopen more quickly.

Full-depth precast concrete bridge decks are one option to help speed up the construction of bridge decks at the bridge site. The deck is cast in segments away from the construction site (Figure 1). This provides good quality control and more flexibility during construction. In addition, there is minimal work done on the job site and large concrete placements are eliminated from the field. Panels may be lifted directly from a truck and placed on the beams. The panels are placed in their final positions and a minor amount of formwork is placed around the haunches and connections. The panels are then connected to the beams and to each other (Figure 2). Using precast deck panels should limit the amount of construction needed on the bridge site and reduce the disruption to the public.



Figure 1. Constructing Precast Panels at a Precast Plant

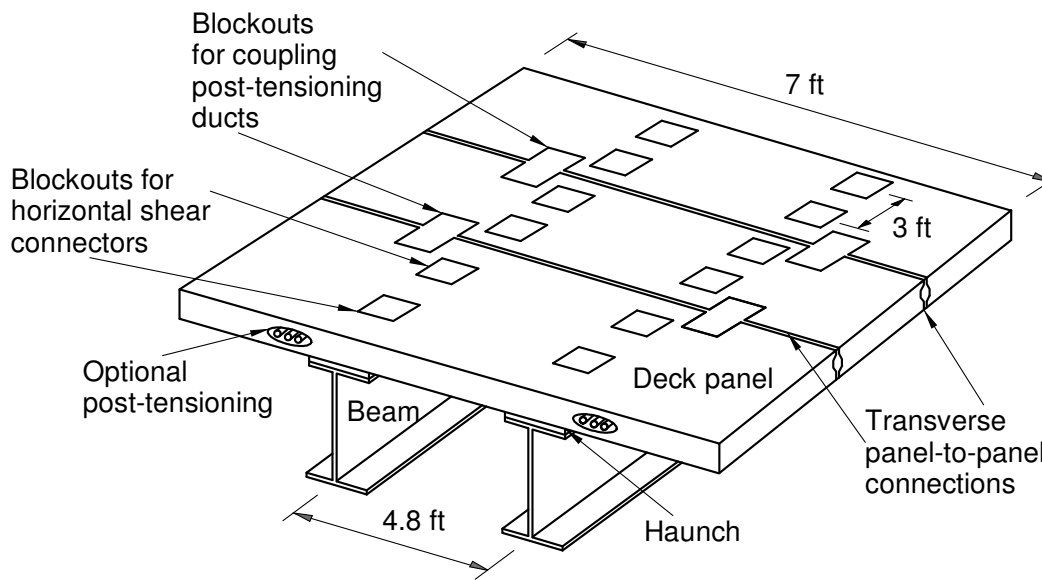


Figure 2. Deck Panel Layout

A hindrance to the widespread implementation of precast deck panels is the lack of guidance for designers. There is remaining uncertainty with respect to design procedures for deck panels and research is ongoing (Swartz, 2008). When using precast parts, there are numerous new connections that must be designed on a bridge deck. As noted by Issa et al.: “The joints are important because bridge deck performance is manifested in the behavior of its joints” (Issa et al., 1995). Connections are a primary cause of deterioration on bridges, and therefore are a big concern for engineers. In addition, the traditional methods of attaching cast-in-place decks to bridge beams with shear studs must be adjusted or changed. Past performance of bridges with deck panels has not been satisfactory in many cases because of faulty designs and bad detailing of the connections.

PURPOSE AND SCOPE

The purpose of this investigation was to systematically evaluate the serviceability response of various panel-to-panel and panel-to-beam connections and grouting methods in a precast concrete deck panel system through laboratory testing. The final step of the research process was to make recommendations for a bridge deck design with precast deck panels based on the results of this research.

To accomplish the goal of implementing deck panels on a wider scale, a literature review was undertaken (Swenty, 2009) to examine previous research on deck panels and to determine areas that needed further investigation. This research project was designed to address many of these problems. The problems are as follows:

1. There is a lack of construction data to support the use of deck panels. Previous uses of deck panels have been undertaken with the assumption that deck panels are economical, but actual data on a project would help provide a basis for comparison.
2. Shear stud pockets are widely accepted, but the grouts and surface preparations have not been widely studied. Within the Virginia Department of Transportation (VDOT), a set of specifications has been formulated, but they should be further tested. The preparation, construction, and design procedures for these pockets should also be monitored.
3. Panel-to-panel connections have always been a problematic area on deck panels. A number of different post-tensioned and reinforced transverse connections have been implemented. Previous testing programs have not investigated connections in negative moment regions on continuous bridges.
4. Post-tensioned connections have been stressed to different levels based on analysis models. There is limited information on the best method to use for the design of post-tensioning stresses in bridge decks.
5. Many tests have focused on the initial stiffness and deflections of deck panel systems on simply supported beams under short-term loads. Few tests have investigated the loss of stiffness and increase in deflections after cyclical negative moment loading.

Based on the literature review, the following objectives were established:

1. Determine which panel-to-panel connection techniques will crack the least and be most durable under the worst-case negative moment service load condition.
2. Determine the level of longitudinal post-tensioning stress in deck panels that is necessary to keep the deck and connections in compression during cyclical testing.
3. Determine the types of surface treatments that prevent or limit cracking and water leakage in the shear stud pockets.

4. Evaluate how the flexural stiffness changes over time in deck panel systems with different types of panel-to-panel connections.
5. Determine which construction techniques work best when building a full-depth precast bridge deck.
6. Document the material and labor costs to build the laboratory deck panel specimens.

To achieve the stated objectives, the study investigated post-tensioned and mildly reinforced panel-to-panel connections, shear stud pocket surface treatments, and construction procedures for full-depth precast concrete deck panels in a laboratory setting. Three specimens were used. Each comprised two steel beams supporting three precast panels with two panel-to-panel connections and twelve shear stud pockets. The three-panel specimens were tested in negative bending under cyclical loading for 1,000,000 cycles. Both prestressed and non-prestressed connections were compared under the same testing scenario. All of the construction procedures, material quantities, and labor used to build the lab specimens were recorded to help evaluate the overall costs of the various construction methods.

The laboratory research described in this report was followed by the implementation of full-depth precast bridge deck panels for the re-decking of the Rte. 65 Bridge over Staunton Creek in southwestern Virginia. The live load testing and long-term monitoring of this structure are presented in Woerheide (2012).

METHODS

The test procedures used to address the design, construction, and performance issues with panel-to-panel connections placed in continuous composite full-depth precast bridge deck panels and to investigate surface preparation techniques for horizontal shear connector block-out pockets are discussed in the following sections. The results of the tests were used to produce recommendations for the selection and construction of panel-to-panel connections and guidelines for constructing the grouted shear pockets.

Panel-to-Panel Connections Investigation

Panel-to-Panel Connection Selection and Design

Three panel-to-panel connection reinforcement configurations for full-depth deck panels were chosen for direct comparison. The connection configurations were chosen based on their use in previous construction and research projects. Of the six connections tested, two incorporated mild reinforcing bars and four included post-tensioned strand (Figure 3). The drop-in bar connection is similar to non-prestressed connections tested on a simply supported bridge by Badie and Tadros (2008). A section of a hollow structural steel (HSS) tube is cast into the panel adjacent to the panel edge to create a slot into which a bar can be dropped across the

narrow keyed connection. The looped reinforcing bar connection is similar to numerous mildly reinforced connections used on previous bridges (New England Region PCI, 2002). The post-tensioned connections were designed with shear keys and post-tensioned strands.

Four replicates of the post-tensioned connection were tested; each had the same geometry, but two had neat grout, one had a pea gravel–extended grout and one had an epoxy bonding agent between the grout and concrete interface. In addition, the first neat-grouted connection and the pea gravel–grouted connection had different levels of post-tensioning stress applied than the second neat-grouted connection and the epoxy-treated connection. Every connection was designed to carry the same worst-case negative bending moment over an interior support. The tests provided information to directly compare the performance of the connections. The six connections were named as follows:

1. Drop-in Reinforcing Bar Connection
2. Looped Reinforcing Bar Connection
3. Post-Tensioned Neat Grout – 167 psi
4. Post-Tensioned Pea Gravel Extended Grout – 167 psi
5. Post-Tensioned Neat Grout – 340 psi
6. Post-Tensioned Neat Grout Epoxied Faces – 340 psi.

The continuous three-span bridge in southwest Virginia that carries Rte. 65 over Staunton Creek provided the basis for the design of the test setup and panel-to-panel connection specimens (Figures 4 and 5). The selected bridge represented a typical layout for a steel beam bridge in need of a new deck. The bridge is owned and maintained by VDOT. The superstructure layout for the project included W21×83 beams spaced at 4.8 ft, an out-to-out deck width of 30.3 ft, and a composite three-span design (31 ft - 32.5 ft - 31 ft). The bridge has one 12-ft lane in each direction, a 2-ft shoulder on each side, and a Kansas Corral barrier rail.

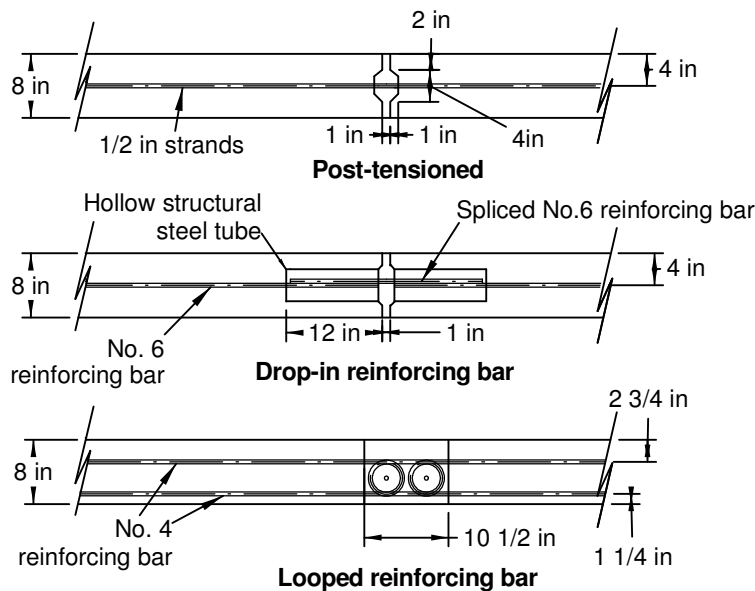


Figure 3. Sections of Alternative Transverse Connection Details

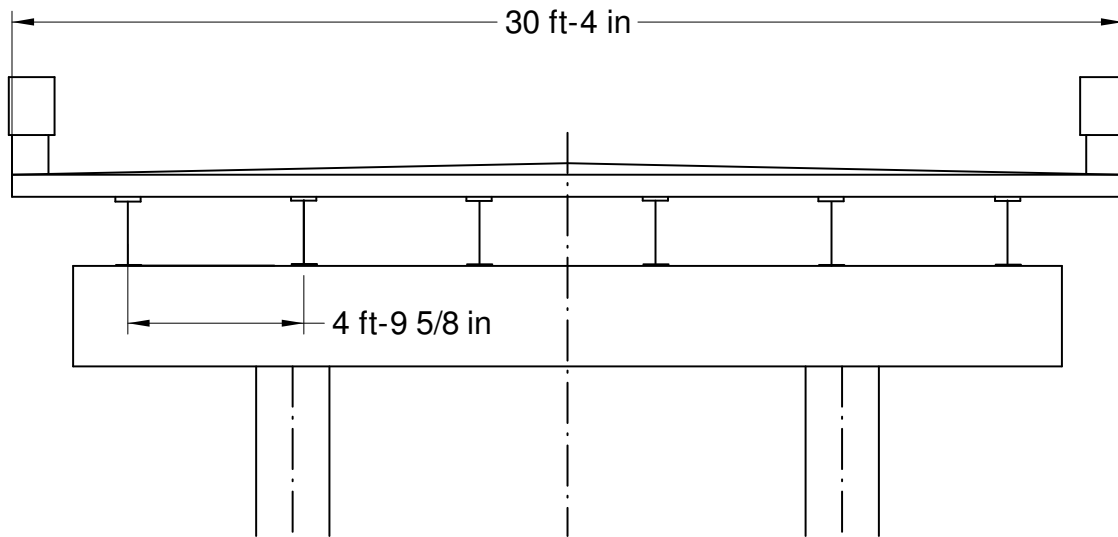


Figure 4. Transverse Section View of the Virginia Bridge

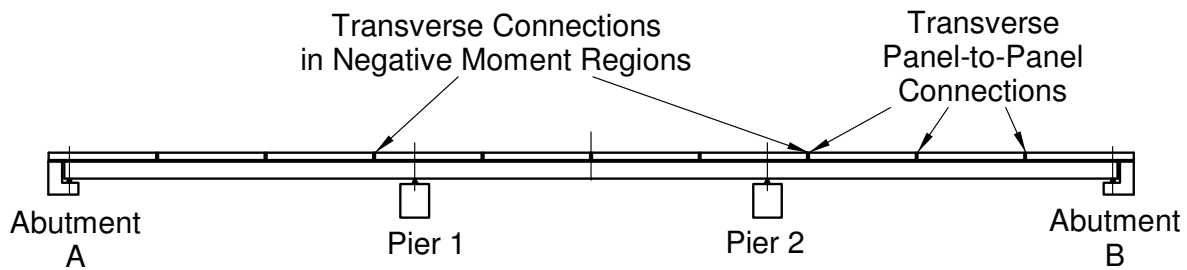


Figure 5. Longitudinal Elevation View of the Virginia Bridge

After the transverse connections and bridge for re-decking were chosen, the panels were designed. The focus was on the continuous, composite region over the interior bents where the connections would experience the highest tensile stresses (Figure 5). The panels were designed following the procedures in the AASHTO Standard Specifications for Highway Bridges using Load Factor Design methodology because VDOT planned to design the actual bridge with these specifications (AASHTO, 1996). The steel beam size was provided by VDOT and was not designed as part of this project.

The bridge was first analyzed to determine the anticipated maximum stresses in the superstructure in the transverse and longitudinal directions when loaded with a standard HS-20 design truck. The HL-93 truck was not chosen because the bridge was to be designed by VDOT with the AASHTO Standard Specifications (AASHTO, 1996). The HL-93 load comprises a distributed lane load combined with that of the HS-20 design vehicle; therefore the stresses would be expected to be higher. The deck was designed using a combination of standard and new methods unique to deck panels. The only deviations from standard bridge deck design methods were on the aspects of design that are unique to full-depth precast bridge deck panels.

Three main differences exist between the design of precast deck panels and conventional cast-in-place decks: transverse prestressing, transverse connections, and shear pockets. The design of these components is not explicitly addressed in the AASHTO Standard Specifications.

The first step was to design the panels with prestressing in the transverse direction. A continuous analysis was done using an HS-20 design vehicle load, with load stepped across the bridge deck in the transverse direction (Swenty, 2009). The supports over each beam were idealized as pin supports. The panels were designed using a 1-ft strip of concrete and two concentric, transverse prestressing strands. The stress levels were checked to ensure the panels met the AASHTO Standard Specification (AASHTO, 1996, Section 9.15.2). This provided a compressive force in the panels during production, transportation, and placement that prevented cracking and provided transverse strength.

Next, the panels and connections were designed for longitudinal bending. An analysis of the bridge was done in the longitudinal direction. The supports at the abutments were modeled as rollers and interior supports were modeled as pins. This was consistent with the actual bridge bearings. The analysis was done assuming an unfactored HS-20 vehicle load using a computer program. The moment envelope from the HS-20 vehicular live loads was recorded and then moments were factored using the load factors from the AASHTO Standard Specification (1996). The post-tensioned connections were designed by stress analysis. The stresses throughout the post-tensioned deck panels were checked to ensure they stayed within the compression and tension limits. The limits from the AASHTO Standard Specification (AASHTO, 1996) were used. All of the connections were designed for strength. A strength analysis was performed on the post-tensioned and reinforced connections to ensure they could carry the factored design moments.

Last, the panels were designed as being composite with the steel beam system. The horizontal shear forces at the girder-to-panel interface were computed; then the steel needed to transfer the force was determined (AASHTO, 1996, Section 10.38.5). The horizontal shear connections were shear studs placed in pockets spaced at 3 ft center-to-center along the girders. The shear pocket dimensions were chosen based on the minimum spacing between the shear studs allowed (AASHTO, 1996, Section 10.38.2.4). The spacing of the shear pockets was chosen based on a 4-ft maximum recommended from previous research (Sullivan and Roberts-Wollmann, 2008) and on geometric limitations within the panels. A rectangular pocket shape was chosen because it has been used in previous projects, as shown in the literature review. Full details of the deck design and panel drawings can be found in Swenty (2009).

Panel-to-Panel Connection Testing

Following the design of the complete deck system, the negative bending test was devised. The test was modeled after the interior supports on the Virginia Bridge (Figure 5). The goal was to test full-size transverse connections under cyclical, service loads. All testing was performed at the Virginia Tech Thomas M. Murray Structures Laboratory.

To use resources efficiently, the testing focused only on a section of the bridge with transverse connections. A full-scale, two-beam portion over an interior support was chosen for

testing. Everything on the models was kept similar to the bridge deck design to limit the number of variables among the tests. Shear studs were welded in pockets, which had a uniform spacing of 3 ft. The stud pattern is shown in Figure 6. The bridge deck depth was 8 in, and the beam spacing was 4.8 ft for all specimens. For simplicity, a uniform haunch height of 1.5 in was used throughout to simulate a typical situation. The design compressive strength of the concrete used in the panels was 5,000 psi. The beams used in the test were W21×101, instead of W21×83, because of easy availability (Figure 7).

The laboratory test setup was a double-cantilevered system symmetric about the center support (Figure 8). A load was applied at one end with a hydraulic servo controlled actuator. The load frame was built using two W12×58 shaped columns bolted to the strong floor and a double channel C15×50 beam connecting the columns. The other end was tied down with eight 1-in threaded tension rods (Figure 9). The midpoint of the bridge had a steel roller under each beam. Because of the symmetry of the loads in the system, two connections were tested simultaneously. The specimen had connections spaced at equal distances from the center support.

The specimen was designed to test the full-scale panel-to-panel connections under the maximum stress caused by an HS-20 vehicle. Using the maximum moments computed from the connection design, a stress level in the panels over the interior bents was computed. The stress levels in the connections during testing were designed to be the same as the stress level produced by the design loads on the real bridge. The stress range for the connection was created by cyclically applying a 75.5-kip force to each cantilever at 5.5 ft from the centerline of the transverse connections. A sinusoidal load was applied at a rate of 1 Hertz throughout the cyclical tests. The service load range for the cycles was 0 to 75.5 kips but the actual load varied between 2.5 kips and 78 kips. The testing matrix is shown in Table 1. Specimen plan views are shown in Figures 10 and 11.

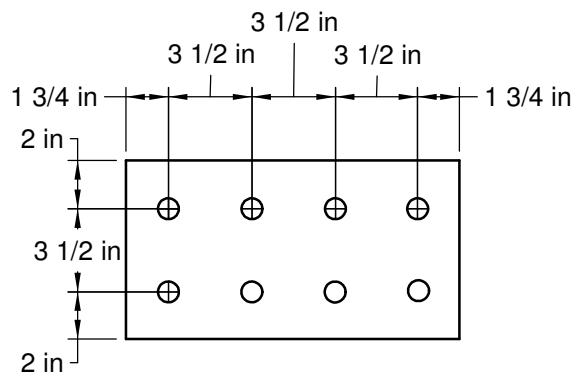


Figure 6. Shear Stud Layout in Block-out Pockets

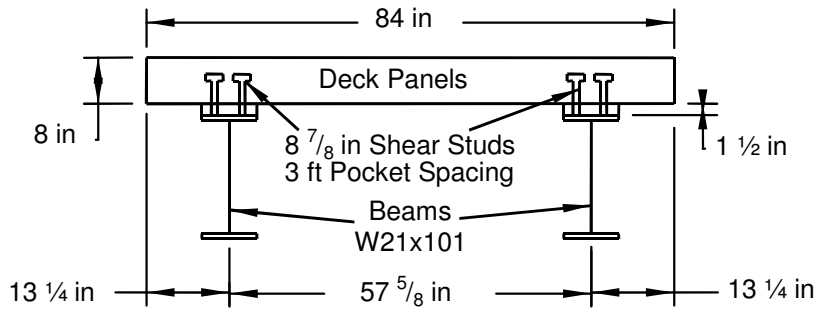


Figure 7. Composite Connection Between the Panels and Beams (End Elevation View)

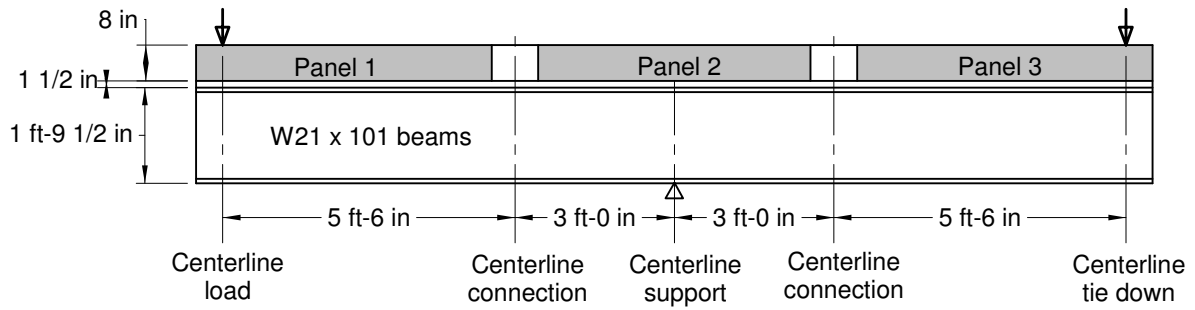


Figure 8. Testing Setup (Elevation View)



Figure 9. Panel-to-Panel Connection Test Setup

Table 1. Panel-to-Panel Connections Testing Matrix

Specimen	Connections Tested
Reinforced Connections	Drop-in Reinforcing Bar Connection Looped Reinforcing Bar Connection
Post-Tensioned Connections 1	Post-Tensioned Neat Grout- 167 psi Post-Tensioned Pea Gravel Extended Grout-167 psi
Post-Tensioned Connections 2	Post-Tensioned Neat Grout-340 psi Post-Tensioned Neat Grout with Epoxied Faces-340 psi

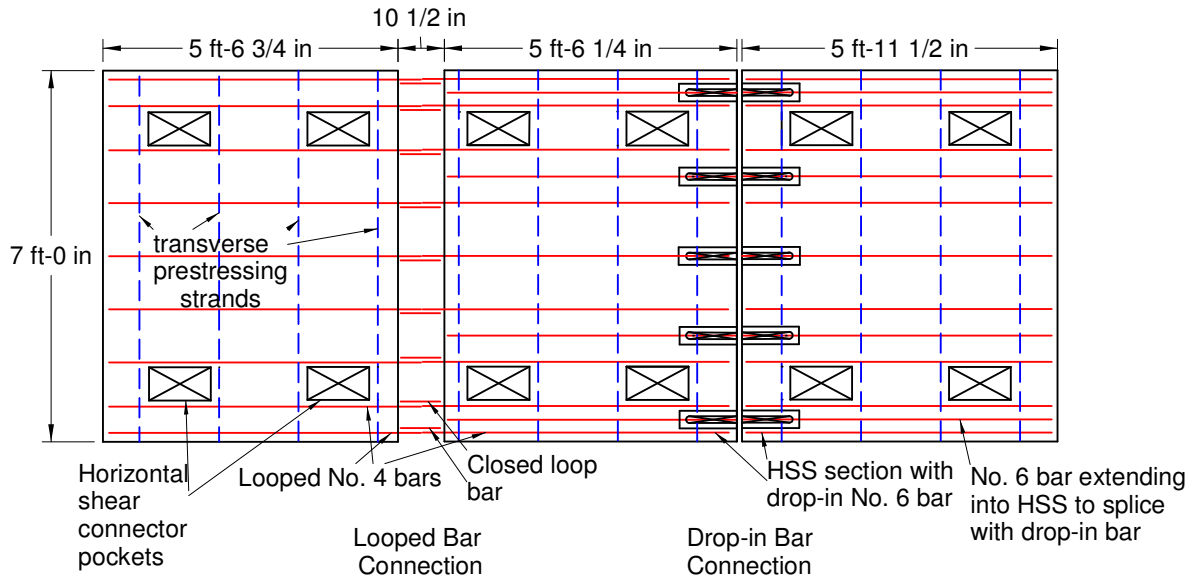


Figure 10. Specimen with Reinforced Connections

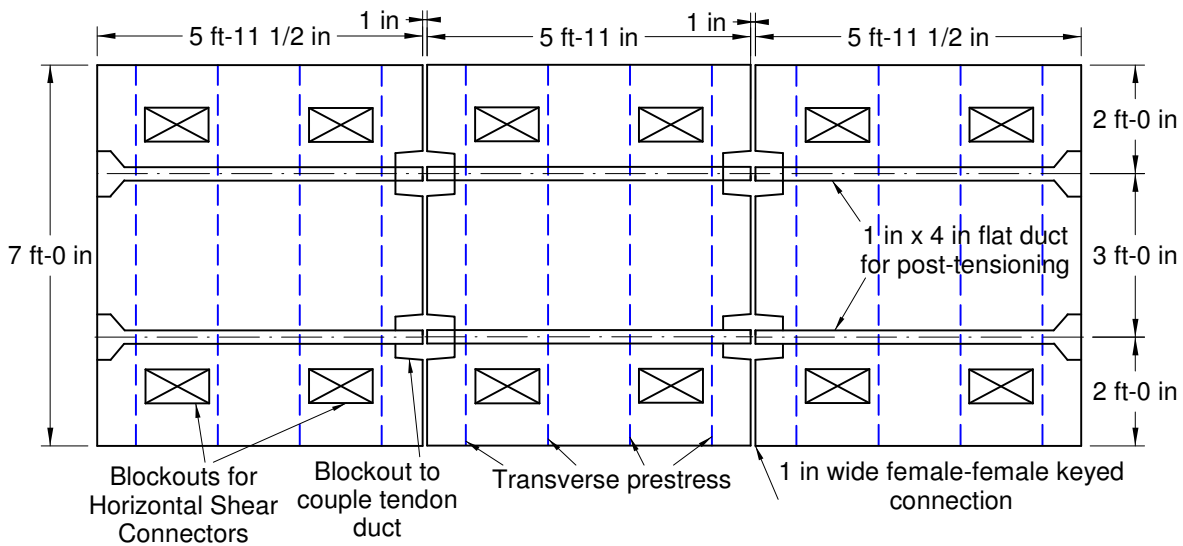


Figure 11. Specimens with Post-Tensioned Connections

Construction Study on the Panel-to-Panel Connection Tests

Many of the steps used in the construction processes contribute to the performance of the deck panels, as documented in the literature review. In the tests presented here, the construction of the precast panels and the transverse connection tests were carefully documented. The observations started in the precast panel plant and continued through the end of testing in the laboratory.

The first part of the construction process was done in the precast plant of the Shockey Precast Group in Winchester, Virginia. This precast plant was chosen because of its relative proximity to the testing lab and their employees' experience at making precast parts. The panels were built in outdoor stressing beds with an awning covering the construction area. The locations of different panel components, including the post-tensioning duct, the leveling bolts, and the prestressing strands, were monitored. Vibrating wire gauges (VWGs) were installed at the edges inside the panels during this process (Figure 12). These were used during testing to determine the strains in the top of the panels at mid-span. Concrete cylinders measuring 4 by 8 in were made for strength and modulus tests.

After the panels were made and delivered by truck, construction began on the test specimens. The construction process in the laboratory had a number of unique steps that are performed differently on standard cast-in-place concrete decks. Particular attention was paid to processes that have no widely accepted method, as demonstrated in past literature. This included:

1. forming the haunches
2. leveling the panels
3. forming the connections
4. grouting the deck
5. post-tensioning the panels.

The haunches were formed between the panels and steel beams to keep the grout in place during placement. In the first test setup, two methods were used to form the haunches: fiber forming board and cold formed steel angles (Figure 13). The fiber forming board was made of recycled paper fiber. The board was purchased in 1/2-in-thick sheets, cut to size, and glued together. A 1 1/2-in-thick haunch was used throughout. The boards were then glued to the outer edge of the top flanges of the beams. The second material used was a cold formed steel angle with leg dimensions of 1 1/2 in. A 1/4-in-diameter tie rod was used at approximately 4-ft spacing along the beam to provide transverse support. The bottom leg of the angle was glued to the top flange of the beam to ensure stability during construction. Prior to putting the panels in place, a small strip of weather seal was placed on the top edge of the flange of the angles. Observations were made of the ease of construction and effectiveness at containing the grout. In the last two setups, the fiber forming board was used throughout.



Figure 12. Installing the Vibrating Wire Gauges in the Panel

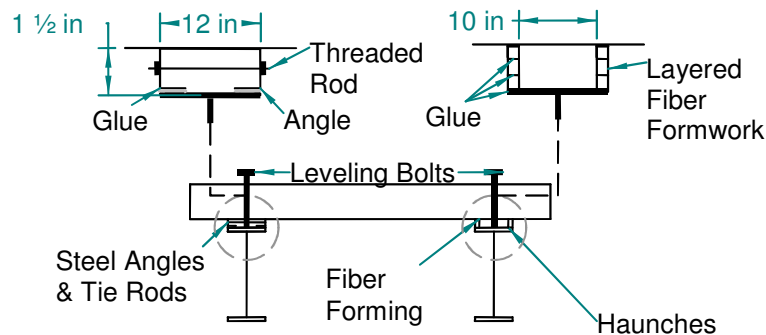


Figure 13. Bridge Haunches

After the haunches were formed, leveling bolts were installed in the panels and the panels were lifted into place using a crane. The leveling bolts were used to adjust the height of the panels. This is a method that has been previously reported for deck panel construction. There were three inserts for $\frac{3}{4}$ -in diameter bolts cast into each panel. On one side, the single bolt was at the center of the panel over the beam. On the opposite side there were two bolts, positioned just outside of the horizontal shear connector block-out. The three inserts can be seen in Figure 12. The bolts were installed with a protrusion of approximately 4 in from the bottom of the deck panels. The bolts rested on the beams while the panels were put into place with cranes. The bolts were then adjusted with a hand wrench to lower the panels to the final elevation. Care was taken to ensure the panels touched the haunch formwork but did not damage it.

Wooden formwork with threaded tie rods was used for all of the transverse connections (see Figure 14). A liquid adhesive was applied around the connections between the wood and concrete to ensure the grout would not leak. The time and ease of construction were monitored. After the grout cured, the wooden formwork was removed but the tie rods were left in place. In five of the six connections, the tie rods left weak spots that extended through the entire depth of the connections. In the looped reinforcing bar connection, the reinforcing within the connection was used as support for the bottom formwork. This method was devised to prevent protrusions in the top surface of the grout (Figure 15).

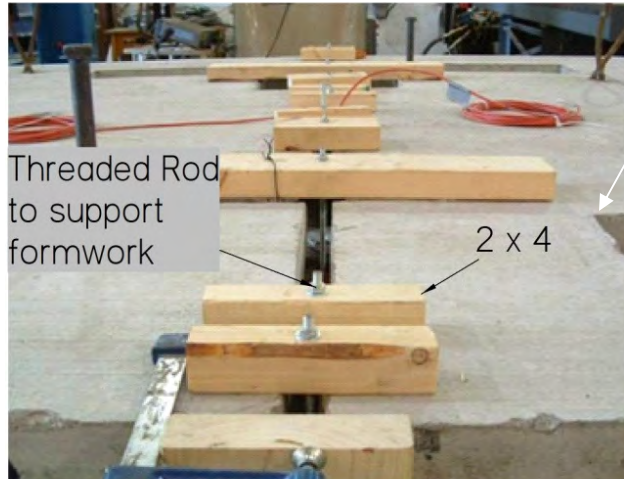


Figure 14. Formwork for the Narrow Transverse Connections

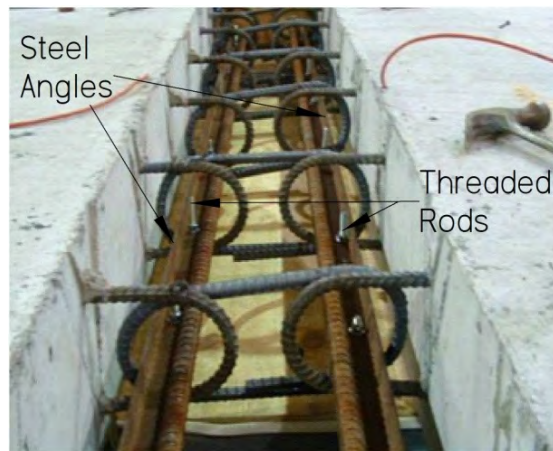


Figure 15. Formwork for the Wide Transverse Connections

A highway patch grout was used in all connections, haunches, and shear pockets. The grout is typically used in bridge deck rehabilitation projects for patching deck surfaces. Previous research showed that this type of grout had good performance characteristics, such as good flow, good bond, low shrinkage and high early strength, for deck panels (Scholz et al., 2007). Mixing procedures followed the recommendations of the manufacturer. On one transverse connection the grout had an additional $\frac{3}{8}$ in nominal maximum size pea gravel extension as allowed by the manufacturer. Differences between the construction of the grout with and without the pea gravel were monitored. Workability and strength characteristics were documented for each batch of grout.

The non-prestressed connections required one continuous grout placement. The transverse connections, haunches, and shear pockets were all interconnected and grout was placed down the beam lines. First the grout was placed in the first shear pocket and continued in this pocket until grout exited through the haunch into the next shear pocket along the beam line. This process continued in each pocket along the beam line (Figure 16). When a transverse connection was encountered it was filled in the same manner as the shear pockets. At the end of the beam line, a 1-in exit hole was left open until the grout flowed out. The hole was then capped.

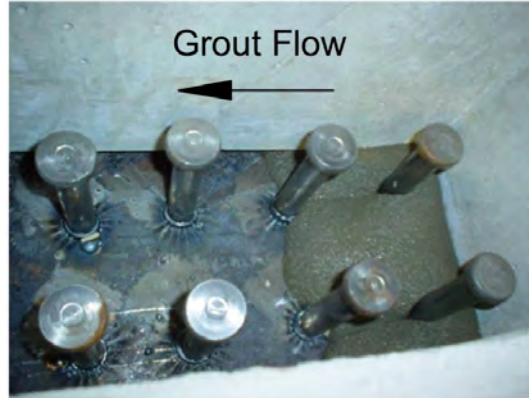


Figure 16. Grouting Along a Beam Line

The post-tensioned connections required three separate grout placements. First, the grout was placed in the transverse connections. Once the grout reached 4000 psi compressive strength, the formwork was removed and the post-tensioning was applied to the deck panels. After the post-tensioning was stressed, the ducts were filled with grout using a grout pump. The grout was pumped through a grouting tube at one end of the post-tensioning duct. Grout was pumped until it came out of the grouting tube at the other end of the post-tensioning duct. The final grouting procedure was to fill the shear pockets and haunch with grout using the same procedure followed in the non-prestressed connections.

In two of the specimens, post-tensioning was applied to the deck in the longitudinal direction. This involved an additional procedure that took extra time. Extra care was taken to safely stress the strands to the correct level without injuring anyone or damaging the laboratory equipment. In both tests, there were two ducts centered at mid-depth in the panels. The ducts were situated 24 in from the outer edge of the panels (Figure 17). In the first set of post-tensioned panels, there were two ½-in super strands in each duct. In the second set of post-tensioned panels, there were four ½-in super strands in each of the ducts.

One load cell was placed on the dead end of one strand in each duct (Figure 18). The load cells ensured that the load in the strands was correct and provided data to back-calculate friction losses. The strand with the load cell was stressed first so that elastic shortening losses from subsequent stressing could be monitored. After post-tensioning, the ducts were grouted as described previously. The additional time and labor needed to add post-tensioned strands were measured.

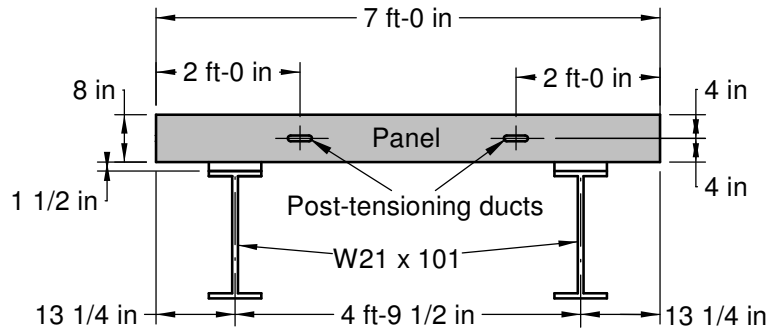


Figure 17. Elevation View of the End of the Transverse Connection Tests



Figure 18. Load Cell on the Dead End of a Strand During Stressing

Transverse Connection Instrumentation and Data Collection

The transverse connection testing consisted of applying a load equivalent to an HS-20 vehicle 1,000,000 times, to emulate the estimated design life of the Virginia bridge. The Virginia bridge had an average daily truck traffic of 50, so over a 50-year service life, the interior supports would experience just under 1,000,000 large negative moment events. The maximum stresses were 540 psi and 100 psi tension at the top and bottom of the deck, respectively. At predetermined points in the test, the cycles were stopped and data was taken during a static test (Table 2). Strains were monitored at the bottom and top flange, midpoint of the beam, and top of the slab. Any cracks were recorded and measured and ponding was performed at intervals on the surface of the decks. Good connection behavior was defined as little cracking, no water leaking through the deck, and a linear strain distribution through the depth of the composite section.

Strain measurements were collected during the laboratory tests on a number of parts in the deck system. VWGs were cast in the panels on each side of the connections at the precast plant in order to monitor the strain levels in the deck. Electrical resistance strain gauges were applied on the steel beams beneath each connection at the top flange, bottom flange, and mid-height of the web. Gauge points for a DEMEC (DEmountable MEchanical) extensometer were used to measure any opening of the connections on top of the slab, which is the point of highest expected stress (Figures 19 through 21).

Table 2. Static Load and Ponding Tests During the Cyclical Tests

HS-20 Vehicle Load Cycles	Static Load Tests	Ponding Tests
0	X	X
1	X	X
1,000	X	
5,000	X	
10,000	X	X
20,000	X	
30,000	X	
40,000	X	
50,000	X	X
100,000	X	X
200,000	X	
300,000	X	
400,000	X	
500,000	X	X
600,000	X	
700,000	X	
800,000	X	
900,000	X	
1,000,000	X	X

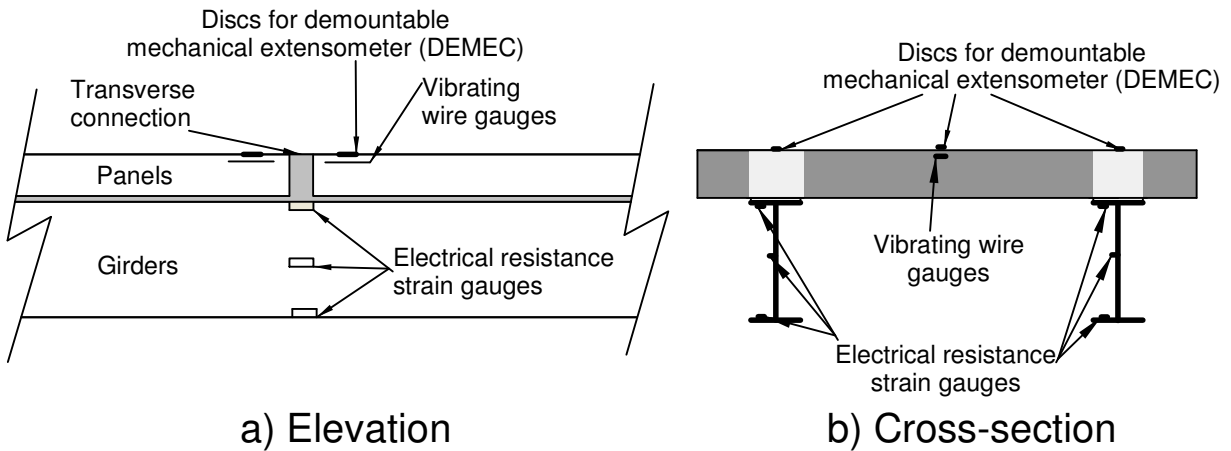


Figure 19. Instrumentation at the Transverse Connections

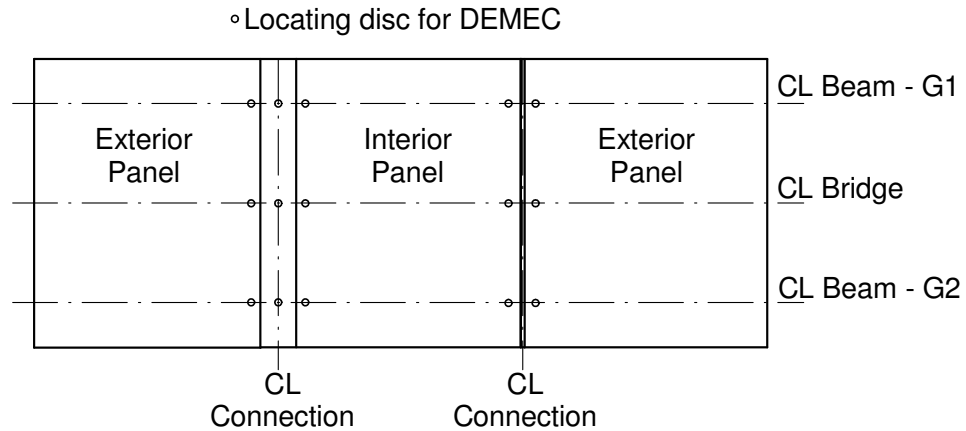


Figure 20. Location of the DEMEC Gauge Points



Figure 21. Taking DEMEC Reading

A ponding test was performed at particular points during the load cycles (Table 2 and Figure 22). A 1-in-high layer of construction adhesive was applied around the edge of the surface of the panels as a dike. Water was then placed on the bridge deck. The ponding test determined when the cracks in the deck were big enough to allow water to flow through the deck over a two-hour time period. No load was applied during these tests, except during the final ponding. After the one-millionth cycle, a ponding test was performed while applying ten service load cycles and then while applying one hundred service load cycles. The bottom and sides of the deck panels were observed for leaks.

As cracks occurred, they were marked on the deck surface. Shrinkage cracks were marked after construction and prior to applying the service loads and documented as non-load-induced cracks. The crack widths, with and without the service load, were measured with a crack gauge at the conclusion of the cyclical loading.

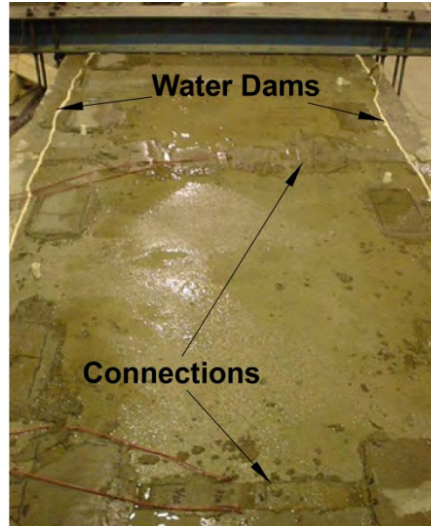


Figure 22. Ponding Test

Horizontal Shear Connector Block-out Pockets

This aspect of the research focused on the surface preparation and grouting procedures used on the shear pockets in full-depth deck panels. The high early strength, non-shrinking highway patch grouts used in deck panels have a tendency to crack over time. The objective was to find a shear pocket surface preparation that effectively limits cracks and leakage at the concrete-grout interface.

Each of the three specimens had twelve horizontal shear connector block-out pockets. Shear studs were welded to the beams in pockets spaced at 3-ft intervals. All of the shear pockets were filled with a grout mixed per the manufacturer's recommendation. The processes to place the grout were the same for all specimens, but the techniques used to prepare the surfaces of the pockets varied. The pockets measured 14 in long by 7.5 in wide by 8 in thick. The amount of grout in these pockets was substantially more than the amount used in most transverse connections or in typical bridge patching applications. The large volumes of grout placed in the shear pockets created a higher probability of cracking.

For the first two sets of panels, water was applied to the pocket surfaces to maintain a moist condition and grout was placed per the manufacturer's guidelines. After the grout was placed, the pockets were monitored for shrinkage. Monitoring continued on the panels while the transverse connection loading tests were performed. Cracking was labeled on the deck panel top surface and the widths were measured by comparing them to crack gauges (0.005 in or greater). The time from placing the grout to the end of testing for the first and second tests was 42 days and 52 days, respectively.

For the third set of panels, six new surface preparation techniques were chosen for the block-out pockets. In addition, the pockets were ponded with water and monitored for leaks. The goal was to find a better preparation method for the horizontal shear pockets that limited cracking and leaking.

Two pockets with each surface preparation technique were built for a total of 12 shear pocket configurations. Two control pockets were built following the manufacturer’s guidelines by moistening the surface prior to applying the grout. Two pockets were built with each of the following surface treatments: epoxy-coated, sand-blasted, exposed aggregate finish, and grouted surface (Figure 23). The last set of two pockets had water stops placed in the pocket to prevent water from penetrating the deck. Water stop is an extruded plastic element typically cast in place across construction joints to prevent water leakage. The test matrix for the shear pockets is shown in Table 3.

Three of the techniques required additional work from the precast manufacturer. The exposed aggregate pockets were treated with a set retarder prior to placing the concrete. When removing the forms, the pockets were sprayed with water to remove the paste. Sand-blasting was performed on two pockets immediately after removing the formwork. It is noted that the sand-blasting took place 49 days before the grout was placed in the shear pocket. The water stops were placed inside the pocket formwork and cast into two shear pockets. The construction diagrams are shown in Figure 24.

Table 3. Test Matrix of Block-out Pocket Surface Treatment

Pocket Surface Treatment	Reinforced Connections (Number of Pockets)	Post-Tensioned Connections 1 (Number of Pockets)	Post-Tensioned Connections 2 (Number of Pockets)
Moist (Control)	12	12	2
Epoxy-Coated	0	0	2
Sand-Blasted	0	0	2
Exposed Aggregate	0	0	2
Grouted Surface	0	0	2
Water Stop	0	0	2

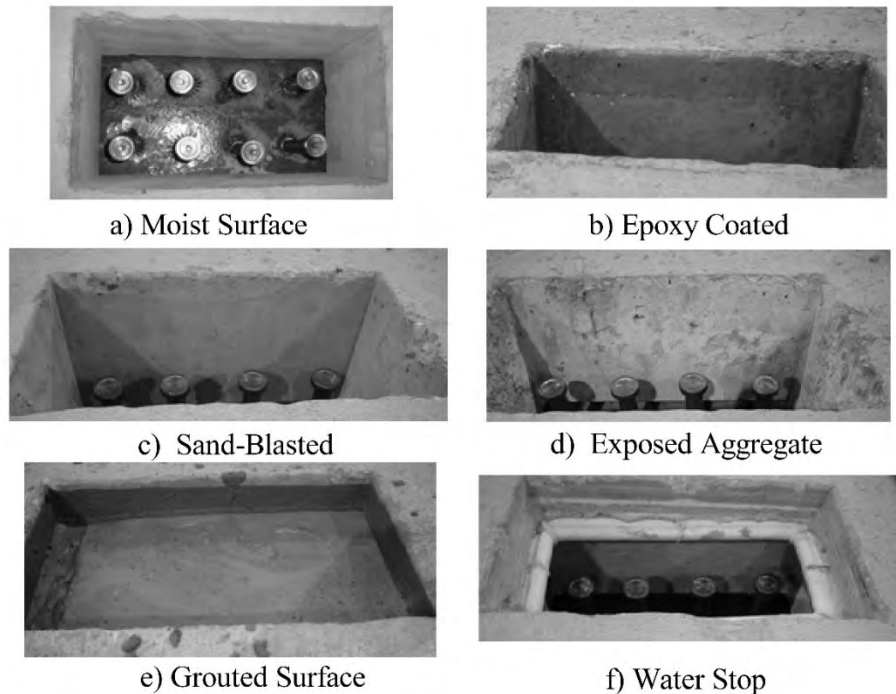


Figure 23. Shear Pocket Surface Preparation Methods

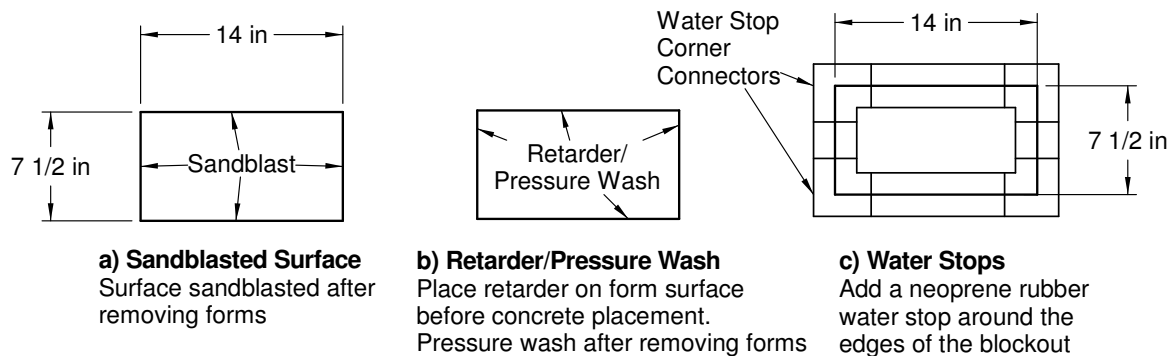


Figure 24. Shear Pocket Construction Notes

Three of the surface conditions required additional work prior to placement of the grout.

1. The epoxy coating was added approximately 30 minutes before the grout was placed, as required by the maker of the bonding liquid epoxy (a vinyl acetate emulsion). The epoxy had a “tacky” feel when placing the grout.
2. The grout paste was applied approximately 15 minutes before grouting two pockets. An approximately ¼-in layer of grout was placed on the inner surface of two pockets. The mix proportions of the grout were the same as the manufacturer’s guideline. The surface grout was still moist when the pocket grouting began.
3. The wetting of the surface in the last two pockets took place approximately 10 minutes before placing the grout. This method was the same one used on the first two sets of panel tests.

The pockets were monitored for cracking in and around the grout. Cracks were marked on the panel and grout surface starting at construction and continuing through the end of the cyclical loading. The crack widths were recorded if they were large enough to be measured with a crack gauge (0.005 in or greater). The time from grout construction through the end of testing was 67 days.

Ponding tests were also performed on each shear stud pocket. First, a barrier was formed around the deck with a 1 in tall layer of construction adhesive. After the adhesive dried, water was applied inside the barrier to a depth of about ¼ in. Only the exterior edge of the shear pockets was visible on the bottom of the panels near the edge of the haunch. Leaks were observed only on this outer edge since the other edges were not visible. Any other cracks that appeared and leaked were also noted.

RESULTS AND DISCUSSION

Three specimens, comprising six connection configurations, were built in sequence and improvements were made as needed during the construction process. The names of the three specimens were as follows:

1. Reinforced Connections –Drop-in Reinforcing Bar
 Looped Reinforcing Bar
2. Post-tensioned Connections 1 – Post-tensioned Neat Grout–167 psi
 Post-tensioned Pea Gravel Extended Grout–167 psi
3. Post-tensioned Connections 2 – Post-tensioned Neat Grout–340 psi
 Post-tensioned Neat Grout with Epoxied Face –340 psi.

The results of the transverse connections tests were fourfold. First, the final designs are reported. The designs included the final effective stress level, after short-term losses for post-tensioning, and the reinforcing bar layout for non-prestressed connections. Second, all of the main steps used to build the setup were documented along with the amount of time and human resources needed. The effectiveness of the various techniques was also observed. Third, the durability of the connections was measured through cracking and ponding observations. Last, strain profiles through the depth of the composite section were created at the transverse connections and deflections were measured.

Transverse Connection Design

Six unique transverse connections were designed. The beam composite section at the connection was designed for a factored moment of 587 kip-ft, the design moment over an interior pier on the Virginia bridge. The design strength of the composite cross-section with the looped reinforcing bar connection was 754 kip-ft, with looped No. 4 reinforcing bars spaced at 10 in. The drop-in bar connection had similar design strength of 735 kip-ft with No. 6 reinforcing bars spaced at 18 in. The strengths were higher than required due to the use of a larger W-shape than the design required. The strength calculations were done using the AASHTO Standard Specifications to meet the requirements of VDOT.

A parametric study was conducted on the level of prestressing in a full-depth precast panel system by Bowers (2007). The result was a list of recommendations for stress levels in the panels. For a post-tensioned three-span continuous beam system, a design value of 500 psi was recommended.

To test the design method used for this stress recommendation, two stress levels were used on the two post-tensioned specimens. The goal was to design the first set of panels with the absolute minimum amount of stress needed. The panels were designed with the same maximum design service moment used for the non-prestressed connections (266 kip-ft). The maximum allowable tensile stress permitted in the top of the concrete deck under the service load was 0.42 ksi. This was based on a tensile limit of $6\sqrt{f'_c}$ (f'_c in psi) using a design f'_c value of 5000 psi. The estimate was conservative compared to the $7.5\sqrt{f'_c}$ (f'_c in psi) stress allowed in the ACI 318-08 design code ((ACI 318 2008) Section 18.3.3). The estimate was also conservative compared to the $0.24\sqrt{f'_c}$ (f'_c in ksi) stress allowed in the AASHTO LRFD Bridge Design Specifications (AASHTO 2012) Section 5.4.2.6). The assumption was that if enough

prestressing force was placed in the panels, then the tensile stresses would remain low and cracking would be prevented.

The designed stress levels using Bower's model are shown in Table 4 for the Virginia demonstration bridge and the transverse connection test specimens. The rows in the tables are as follows:

1. Steel beam type analyzed
2. Beam spacing
3. Span length (center of support to center of support)
4. Number of strands in the deck per beam line
5. Initial compression in the deck (negative is compression)
- 6.-7. Final deck compression after internal stress redistributions over the design life (negative is compression)
8. Stress at the top of the deck due to restoring forces caused by interior supports
9. Stress at the top of the deck due to the HS-20 truck
10. Distribution factors computed from the AASHTO Standard Specifications
11. Stress at the top of the deck for one beam line (row 9 * row 10)
12. Final Stress in the top of the deck
 - i) For the laboratory specimen (row 5 + row 11)
 - ii) For the Demonstration Bridge (row 6 + row 8 + row 11).

The first four rows of Table 4 present the beam types, beam spacing, and number of strands per beam line for different deck designs on the demonstration and test bridges. Rows 6 and 7 in Table 4 show the anticipated final compressive stress in a simply supported span with no load. The changes in stress occur due to internal stress redistributions as the deck tries to shorten due to creep and shrinkage, but is restrained by the beam. The creep and shrinkage models in the AASHTO LRFD Bridge Design Specifications (AASHTO, 2012) over a 10,000-day design life were used.

Row 8 of Table 4 presents the stress due to the restoring force over an interior support resulting from continuity in the bridge. If there were no interior supports, due to the shortening of the deck caused by creep and shrinkage, the entire bridge would deflect downwards. The interior supports prevent this downward displacement by exerting an upward force on the superstructure. These upward reactions cause negative moments over the interior supports and interior span, which result in additional tension in the deck.

For the demonstration bridge, an analysis was performed on the three-span continuous bridge. The longitudinal analysis considered the end supports as rollers and the interior supports as pins. A longitudinal analysis was done with the laboratory bridge but with the two beam system (7 ft wide) and 18.2-ft cantilever test setup. A restoring force was only computed for the demonstration bridge because it was continuous. The restoring force was not included for the test setup because it was not continuous. The final value was computed for one beam line based on the distribution factor from the AASHTO Standard Specification (column 10).

Table 4. Deck Stress Levels for a Simple and a Continuous Span Bridge

		Lab Bridge		Virginia Bridge			
1)	Beam Type	W21×101	W21×101	W21×83	W21×83	W21×83	
2)	Beam Spacing (ft)	4.8	4.8	4.8	4.8	4.8	
3)	Span Length(s) (ft)	18.2	18.2	32/32.5/32	32/32.5/32	32/32.5/32	
4)	Number of Strands in Deck per beam	2	4	2	4	6	
Results from Simple Span Analysis							
5)	Initial Compression in Deck (psi)	-164	-328	-133	-266	-399	
6)	Stresses after Redirection	Top of Deck (psi)	-129	-281	-138	-268	-394
7)		Bottom of Deck (psi)	-3	-133	-3	-112	-219
Results from Continuous Bridge Analysis – Interior Support							
8)	Stress in the Top of the Deck	Stress from Restraint Moment (psi)			169	194	218
9)		Live Load Stress (psi)	588	588	862	865	863
10)		Distribution Factor (DF)	1	1	0.437	0.437	0.437
11)		LL Stress × DF	588	588	301	302	301
12)		Final Stress (psi)	420	260	330	230	130

(Negative indicates compressive stress.)

For the lab specimens, the final stress expected, shown in column 12 of Table 4, is the sum of the initial effective stress, and the stress due to a live load (HS-20 vehicle). The original target was to keep the final stress levels in the deck below $6\sqrt{f'_c}$, which is 420 psi for the 5000 psi specified compressive strength of the deck panels. The initial stress of 164 psi shown in the first data column of Table 4 was used in the first post-tensioned lab specimen with two strands per beam line. The second laboratory specimen had four strands per beam line, which resulted in an initial stress of 328 psi. The final stress with live loads was expected to be 260 psi, or approximately $3.7\sqrt{f'_c}$.

Constructability Evaluation

The construction processes performed in the laboratory are listed in Tables 5 and 6. A summary of all of the materials, manpower, and time needed to perform each task is included. Following is more detailed information on unique processes used for precast panels. This includes the precast panel construction, forming, grouting, post-tensioning, and connections.

Each process performed in the laboratory is broken down into a quantity for the test bridge based on the model's dimensions and layout. The information in Tables 5 and 6 was provided to the research sponsor, VDOT, for use in estimating the cost for the demonstration bridge project. Given that the demonstration bridge will have a similar layout on a much larger scale, the quantity per square foot and installation rates per hour were included.

Table 5. Materials Used in the Transverse Connection Construction

Test Bridges 7 ft wide by 18.2 ft long by 8 in deep 2 – W21×101 Beam Lines			
Lab Materials	Quantities	Description	Quantity/ft ²
Grout		50 lb Bags	0.32 (Post-Tensioned Option)
in Post-Tensioned Connection	6		
in Pea Gravel Extended Post-Tensioned Connection	3		
in Looped Connection	10		
in Drop-in Bar Connection	7		
in Ducts	4		
in Haunches	23		
Strands (Oversized)	8	½ in x 32 ft Grade 270	0.06
Formwork	1	½ in x 8 ft x 4 ft sheet of plywood	0.01
	3	2 in x 2 in x 8 ft sawn lumber	0.02
	72	¼ in washer/nut sets	0.57
	36	Feet - ¼ in threaded rod	0.29
B-14 Coil Leveling Bolts	9	¾ in x 14 in	0.07
Haunch Material	72	Feet - ½ in x 3 ½ in fiber formwork	0.57
Shear Studs	96	⅞ in x 5 ½ in	0.76
Ferrules	96	⅞ in	0.76

Observations When Constructing the Panels

The panels were fabricated on two different days at a precast plant: the first two sets of panels, for the reinforced specimen and 167 psi post-tensioned specimen, were built in April 2007 and the third set, for the 340 psi post-tensioned specimen, was built in December 2007 (Figure 25).

Observations at the precast plant were documented to help with future projects. The employees at the precast plant mentioned that the formwork, prestressing strands and reinforcing bars were not hard to install. The difficulties started with the post-tensioning anchor assembly. Closed ties were detailed to provide confinement at the post-tensioning anchorage device. The precast fabricator requested to replace the closed tie with interlocking hairpin bars.

Table 6. Labor to Build the Post-Tensioned Test Bridges

Construction Process	Details	Number of People	Time (Hours)	Installation Rate and Units	
Beam Installation	Installing Haunch Fiberboard	1	3	12.00	ft/hour
Transverse Connection	Making Connection Formwork	2	4	3.50	ft/hour
	Placing Panels	3	3	1.00	panel/hour
	Placing Connection Formwork	3	2	7.00	ft/hour
	Making Haunch Formwork	1	3	1.33	form/hour
	Installing Haunch Formwork	1	1	0.25	form/hour
	Placing Grout	6	1	14.00	ft/hour
	Formwork Removal	1	1	---	
Post-Tensioning (4 Strands per Beam Line Option)	Installing Tendons or Rebar	2	1	144.00	ft/hour
	Stressing Tendons	3	6	1.33	tendons/hour
	Grouting Ducts	5	1	36.00	ft/hour
Composite Action	Shear Studs	2	3	32.00	studs/hour
	Cleaning Haunches	2	1	36.00	ft/hour
	Grouting Haunches	7	2	18.00	ft/hour
Panel Support Release	Removing Leveling Bolts	1	1	9.00	bolts/hour

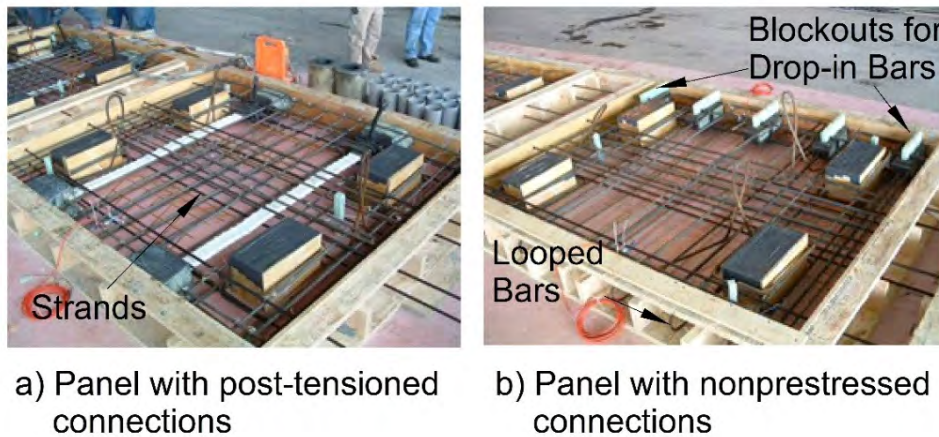


Figure 25. Forming the Panels at the Precast Plant

There were also comments by the precast fabricator on the difficulty of placing the HSS (Hollow Structural Steel) tube sections and post-tensioning ducts at the right location in the panels. The HSS sections were 4 in by 4 in by 12 in long and spaced at 18 in along each joint (see Figure 3). The weight of the steel made the sections hard to stabilize in the formwork. The ductwork was very flexible and was hard to keep at the correct elevation.

The leveling bolt assemblies needed a block-out to install the bolts on the job site, and the HSS sections also required a block-out to form the slot into which the drop-in bar would be placed. Expanded polystyrene foam (EPS) was used on the first set of panels. The EPS above the HSS sections and leveling bolts was very difficult to remove. On the last set of panels, a 1-in-diameter PVC pipe was used for the leveling bolt block-outs. The pipe provided a better quality product, kept the block-outs vertical and the same dimension, and was easier to install.

The water stops for the last set of panels were built by the researchers and given to the precast fabricator to install. The precast fabricator had no problems installing the block-outs, but the workers did comment on the complexity and challenge to build a large number of these assemblies. In general, when pieces had to be suspended in the formwork (ductwork, water stops, HSS assembly), the complexity increased and created problems (Figure 26).

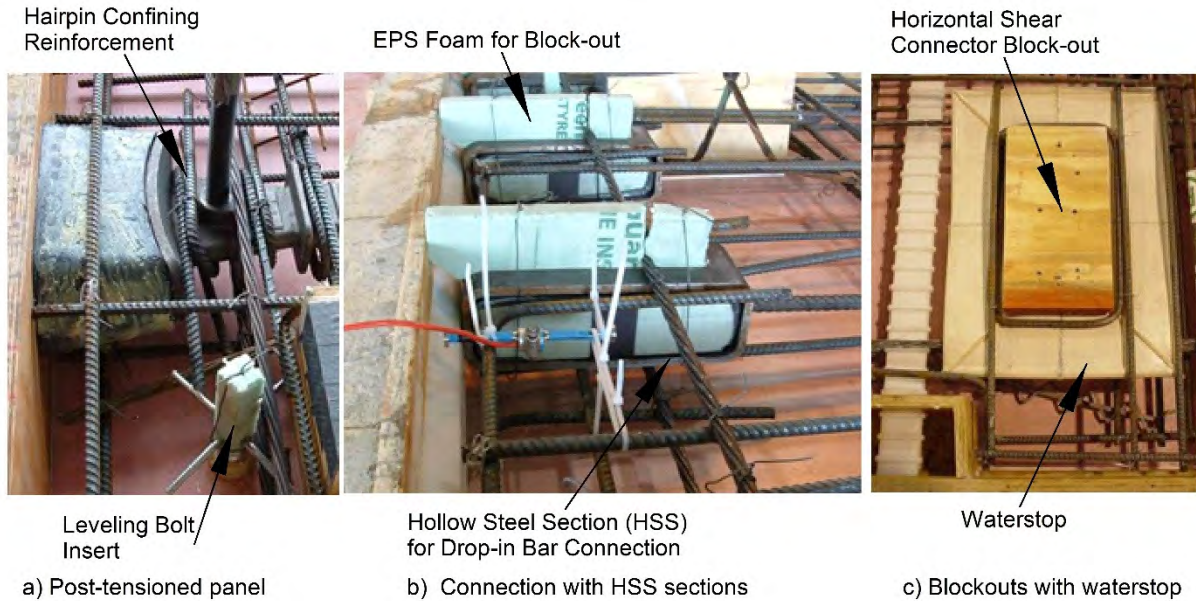


Figure 26. Difficulties Forming Precast Parts

Setting the Beams and Forming the Haunches

Each beam was placed on three support points: the roller in the middle and the temporary support beams on each end. Temporary steel angles were clamped to the flanges of each beam for stability during construction. The top surfaces of the beams were cleaned with a grinder and washed prior to placing the haunch formwork. Two types of haunch formwork were used on the initial setup. The first was a fiber forming board made of recycled paper fiber. The second was the 1.5-in cold formed steel angles tied transversely together with 0.25-in threaded rods. A 1½-in-thick haunch was used throughout (Figure 27).

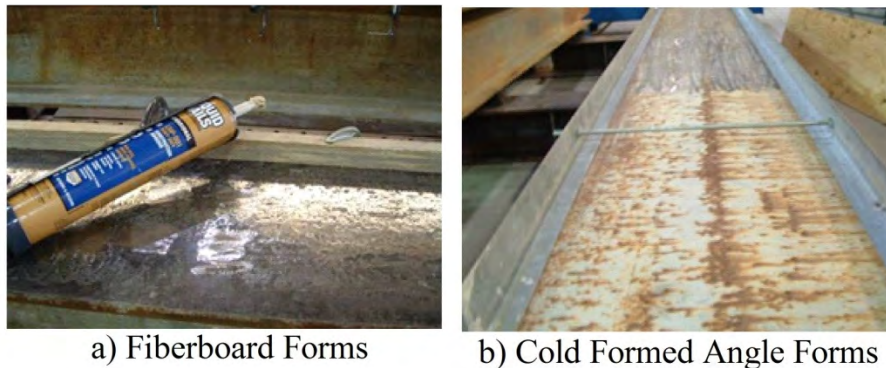


Figure 27. Fiber Formwork and Steel Angle Formwork

The fiber board worked best for the haunch formwork. Cutting, gluing, and placing the fiber formwork was easy and quick, and the material could be cut to height. The cold-formed steel angles provided a good seal, however they were hard to align. Placing the tie rods between the angles took additional time and the angles were difficult to align. The angles did not provide much flexibility with haunch heights unless the angles were cut or bent. In general, this process was harder to construct but took about the same amount of time to setup as the fiber formwork.

Setting Panels and Forming Transverse Connections

Upon arrival at the lab, the first problem was observed on the panels. The EPS foam used as block-outs for the HSS sections and the leveling bolts did not work well. In every location, the EPS was extremely difficult to remove and the leveling bolts were not properly positioned. Many of the leveling bolt locations had to be adjusted with a hand held concrete hammer drill (Figure 28). The HSS sections did not have any concrete inside, however the EPS was hard to remove. A chisel and a propane torch were used to remove the EPS (Figure 29). In the future, the leveling bolt assembly should be used with PVC pipe at the block-outs. The HSS sections should be blocked out with a different material that is easier to remove. A possible option would be to tape around the exterior of the assembly.



Figure 28. Block-outs Around the Leveling Bolt Assemblies



Figure 29. Removing the EPS From the HSS Anchorage Assemblies

The post-tensioning ducts lined up well and the panels were easy to set into place. A few extra minutes were needed to tape each duct together in the block-out regions. Typically, the duct had to be lined up by hand and then taped, but the process worked effectively (Figure 30).

The looped reinforcing bars with the looped connecting bar were easy to place. This connection took a little more time because the bars had to be tied together at a 6-in spacing throughout. However, there was ample space to place the rebar and tie it by hand (Figure 31).

Placing the panels was not difficult with the looped reinforcing bar or post-tensioned connections, but was challenging with the drop-in bar connections. The drop-in bar assemblies were difficult to line up. On the test panel, only two of the five holes for the drop-in bars lined up directly across from one another. The other pieces of reinforcing were forced into the connections and were not perpendicular to the edge of the panel after placement (Figure 32). From a construction standpoint, this connection needs larger tolerances between the reinforcing bar and the embedment.



Figure 30. Coupling Post-Tensioning Duct Across Connection



Figure 31. Looped Reinforcing Bar Tied to Bars Extending From Panel

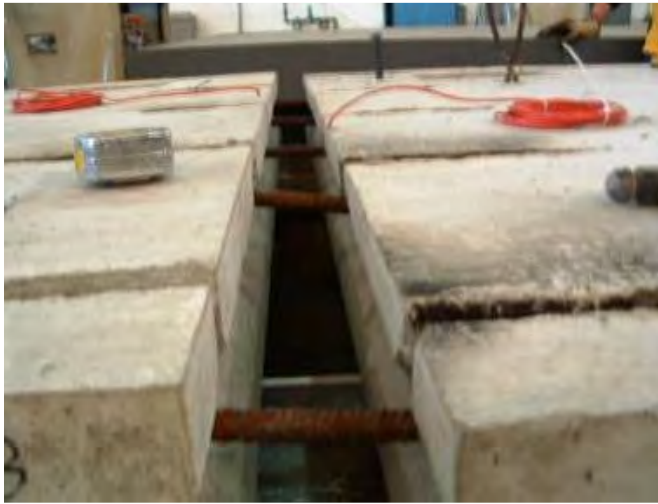


Figure 32. Reinforcing Bars Dropped Into HSS Sections on Opposite Sides of Connection

All of the transverse connections except the looped bar connection were formed with ½-in plywood and ¼-in threaded rods. Typically, the formwork was held in place with 2 in by 4 in pieces of wood on top of the connection and threaded rods (Figure 14). On the looped bar connection, a 1 in by 1 in steel angle was used to hold the bottom formwork. The angles were used to form the connection without leaving holes in the top surface of the transverse connection. The angle was placed through the looped bars on each side of the connection (Figures 15 and 31).

All of these forming techniques worked as expected and kept the grout from leaking out of the formwork. The angles worked especially well because they left no holes in the surface of the panels.

After grout was placed in the haunches, the leveling bolts were removed from the panels. Typically this was done twenty-four hours after finishing the grout. The bolts came out easily by hand with a crescent wrench. For simplicity in the lab, the holes that remained were not filled with grout after removing the bolts, although this would be done in the field.

Placing Shear Studs and Grouting

Grout was placed in the shear stud pockets after the shear studs were welded in the pockets. The pockets had been designed to be as small as allowed by the design code and only provided a couple of inches of space between the shear studs and the walls of the pocket (Figure 33). The process of welding 96 shear studs took approximately one hour for a single experienced welder. The welder commented that the process was not overly difficult. Cleaning the ferrules out of the pockets was the most difficult part after welding the studs. A hand pick was used to break the ferrules off of the studs and a vacuum was used to remove the pieces.

The first grouting procedure was performed on the specimen with the reinforced connections. The panel-to-panel connections, haunches, and shear stud pockets were all grouted in one operation because of the lack of post-tensioning. This grouting on the non-prestressed connections was the largest grout placement of the test program because it encompassed the entire bridge. The grout was very workable for approximately ten minutes. Twenty minutes after mixing, the grout reached initial set. The maximum amount of water recommended by the manufacturer (3 quarts per 50 pounds of grout) was used for the desired flow characteristics. Forty bags of grout were used within 75 minutes to fill all of the spaces. The drop-in reinforcing bar connection was a problem because of the tight space inside the HSS section. A pencil vibrator was used extensively to force grout into the crevices of the HSS section.

Grouting the second and third sets of test panels, the post-tensioned specimens, required more time because of multiple grout pours. The connections between the panels were filled with grout first. The grout was mixed with the maximum amount of allowable water (3 quarts per 50 pounds of grout) and then placed into one end of the connection. Once the end of the connection began to fill, the adjacent section of the connection was filled. This continued until the connection was completely full. Filling the connections was very simple because they were easy to access and required a small amount of grout.

One of the four post-tensioned connections had pea gravel added to the grout (hereafter referred to as extended grout). Thirty-five pounds of a $\frac{3}{8}$ in maximum size river pea gravel was added per the instructions of the grout manufacturer. This almost doubled the output of grout per bag. About $3\frac{1}{3}$ quarts of water were added to each mix instead of the recommended maximum 3 quarts. This decision was made because workability suffered from the introduction of dry aggregate. The aggregate tended to segregate from the grout in the wheel barrow. Care was taken to mix the grout in the wheel barrow to solve the segregation problem. Overall, using pea gravel was not significantly more difficult.

One of the four post-tensioned connections had concrete bonding agent (vinyl acetate emulsion) placed on the panel faces prior to placing the grout in the transverse connection. The epoxy applied to the face of the concrete with a paint brush approximately 30 minutes prior to placing the grout. The epoxy was slightly “tacky” to the touch once the grout was placed, as instructed by the manufacturer. This required careful coordination because the bonding agent could not be permitted to set prior to placing the grout.



Figure 33. Layout of Shear Studs in a Pocket

The second grout stage for the post-tensioned decks, filling the post-tensioning ducts, occurred after the connections were placed, formwork was removed, and the tendons were stressed. The process started slowly but became much easier with experience. A small hand pump worked effectively to fill the ducts with grout. However, in a field deck panel project, an industrial-grade electric pump would be used because pressure grouting is required.

The objective of the last grout placement on the post-tensioned decks was to fill the haunches and shear pockets. This process went very smoothly, mainly due to the experience of the workers. First, the shear studs were welded to the top of the beam through the shear pockets. Like the previous haunch grout placement, grout was placed along each beam line starting at one end. After a pocket was full, the next pocket in line was filled (Figure 34). Grout flowed out of the pockets into the haunch. The flow of the grout was monitored through the shear pockets (see Figure 16). Generally, a vibrator was not required to consolidate the grout; however, for a couple of dry mixes, a pencil vibrator was temporarily used.

Overall, the grouting process was not difficult if the crew had experience. The biggest problem was the set-time of the grout. Having a sufficiently large crew to mix, place, finish, vibrate and make quality control cube samples was essential. Table 7 shows the standard mix proportions used in each grout placement, the respective strengths of the grout, and the conditions at the time of the placement.



Figure 34. Filling the Shear Pockets and Haunches With Grout

A tarp was draped over the panels for the first twenty-four hours but no additional moisture was added to the system. The heat of hydration was very high for the first few hours after the grout was placed and the strength gain was rapid. By the second day, there was no apparent difference in temperature between the surface of the grout and the adjoining panels. The biggest difference between the grout placements was the ambient temperature. As seen in Table 7, the temperature varied greatly from the summer placements to the winter placements.

The strengths varied among the grouts even though the mix proportions remained relatively constant. Some of the variation may have been due to two different batches (from two different orders) of patch grout. The grout was the same brand; however, minor deviations within a brand could have caused some variation. The grout supplier, brand, and storage conditions all remained constant for the test bridges. Grout strength was the primary concern during the connection construction. The strength of 4000 psi was desired for the connection grout before stressing the tendons. The first post-tensioned neat grout was a few psi low, but the remainder of the grouts met the requirement. The strengths all reached 4000 psi prior to testing.

Table 7. Grouting Information

Grout Placement*	Ambient Conditions (temperatures in °F)	Mix Proportions**	Grout Strengths – First Day of Testing
Drop-in and Looped Reinforcing Bar Panels	Afternoon - Clear, Low 60's	2 ¹ / ₃ Quarts / 50 lb Bag	4640 psi
PT Connection Neat Grout– 167 psi	Afternoon – Partly Cloudy, Low 80's, Low humidity	2 ¹ / ₃ Quarts / 50 lb Bag	3970 psi
PT Pea Gravel Extended Grout –167 psi	Afternoon – Partly Cloudy, Low 80's, Low humidity	3 ¹ / ₃ Quarts / 50 lb Bag	4700 psi
PT Connection – 167 psi – Ducts	Noon – Sunny, Low 70's, Low humidity	3 Quarts / 50 lb Bag	4230 psi
PT Connection – 167 psi – Haunches /Pockets	Late Morning – Cloudy, 70's	3 Quarts / 50 lb Bag	6550 psi
PT Connection Neat Grout– 340 psi***	Mid-afternoon – Sunny 45 Outside, 65 Inside	3 Quarts / 50 lb Bag	5360 psi
PT Connection – 340 psi – Ducts***	Early-Afternoon – 50 Outside, 71 Inside	3 Quarts / 50 lb Bag	5170 psi
PT Connection – 340 psi Haunches /Pockets***	Afternoon – Low 60s Outside – Rain, Low 70s Inside	3 Quarts / 50 lb Bag	4800 psi

* PT = Post-Tensioned Panels.

** The maximum recommended dosage was 3 Quarts water / 50 lb Bag grout.

*** Same brand of grout, but a different order from the supplier.

Post-Tensioning

Post-Tensioning Construction

The last four transverse connections were longitudinally post-tensioned. In the first post-tensioned deck, two strands were used per duct (Figure 35). This amounted to a total of four strands in the 7-ft wide bridge deck, or two per beam line. The second post-tensioned deck was the same width, but four strands were placed in each duct (Figure 36). Oversized (super) ½-in strands were used throughout. Threading the strands through the ducts was very easy and only took one person a few minutes per strand.



Figure 35. Two Strands per Duct in the 167 psi Post-Tensioned Connection



Figure 36. Four Strands per Duct in the 340 psi Post-Tensioned Connection

The steel strands were stressed by placing an actuator against a stressing chair. The stressing chair was placed around the anchor assembly and against the end of the panels. The anchor assembly was then accessible for aligning and anchoring the strands (Figure 37). The assembly was easy to use, especially after gaining experience. Two people were needed: one to hold the assembly in place and another to apply the load and monitor the gauges. The hardest part was properly seating the chucks in the anchor. A hammer was used to drive the chucks into the anchor as far as possible to reduce seating losses. Stressing sequence alternated between strands in each duct.

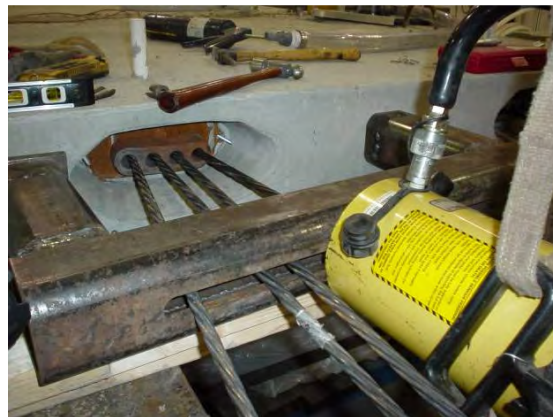


Figure 37. Stressing Assembly

Once stressing began, the load applied to the strands and resulting elongation were carefully monitored. A load-cell was placed on the live end of each strand when the load was applied. Measurements were made of the strand elongation at 5-kip intervals up to the maximum jacking force of 32 kips. This corresponded to 70% of the ultimate strength of the strand ($0.70f_{pu}$). One load-cell was placed on the dead end of the first strand placed in each duct.

For comparison during stressing, expected elongation was estimated for the loads applied to the strand based on elastic deformation equations. Seating losses, elastic shortening losses, and friction losses were included in the estimate. Long-term creep, shrinkage, and relaxation losses were considered, but not measured. They made a negligible difference because testing was scheduled to begin immediately after construction.

Post-Tensioning Force Applied

Calculations were made of the expected losses in the strands during the stressing process and then compared to the actual values. The strands were straight and 19 ft long, so friction and wobble losses were very small. On the first two strands in each setup, a load-cell was used on the dead and live ends (Figure 18). The ultimate jacking force of 32 kips was measured on both the dead and live ends of the strands, indicating little friction and wobble losses.

Seating losses were large because of the short length of the deck (18.2 ft). The first strand had a seating loss of 6 kips because the chucks did not seat well in the anchoring device. As the workers gained experience, the seating losses on subsequent strands were limited to 2 to 3 kips. Elastic shortening losses were computed based on the stressing sequence of the strands. The losses averaged about 1 kip per strand. The biggest losses were measured on the stressing of the first two strands. Subsequent strands had smaller elastic shortening losses.

Table 8 shows the stress level in each strand at the end of the stressing process in the assembly with two strands per beam (post-tensioned 167 psi). Each of these four ½-in-diameter oversized strands ($A_s = 0.167 \text{ in}^2$) was initially stressed to approximately 32 kips. Seating, elastic shortening, and wobble losses were taken into consideration during the stressing process. The average seating loss was about 1.94 kips, or 0.11 in of movement, based on measured movement of the anchors. Elastic shortening values were estimated based on the change in force in the load cells on the dead end of the strand. The friction and wobble losses were estimated based on the difference in force in the live and dead end load cells of the first two stressed strands. The final stress level computed in the panels was 167 psi at the end of the stressing process. The values in Table 8 were all computed based on the values recorded from the load cells and chucks during stressing.

Table 8. Stress Levels in the Post-Tensioned – 167 psi Specimen

	Final Force (kips)	Stress (ksi)	% f_{pu}
Strand 1	25.3	152	56.2
Strand 2	28.0	168	62.2
Strand 3	29.6	178	65.8
Strand 4	28.8	173	64.0
Slab	111.9	0.167	

Table 9 shows the stress level in each strand at the end of the stressing process for the assembly with four strands per beam line (post-tensioned – 340 psi). Each of the eight ½-in diameter oversized strands was stressed to 32 kips ($A_s = 0.167 \text{ in}^2$). Seating, elastic shortening, and wobble losses were taken into consideration during the stressing process. The seating loss on average was about 3.0 kips, or 0.17 in of movement. Elastic shortening values were estimated based on the change in force in the load cells on the dead end of the strands. The friction and wobble losses were estimated based on the difference in force in the live and dead end load cells of the first two stressed strands. The final stress level in the panels was 340 psi at the end of the stressing process. The values in Table 9 were all computed based on the values recorded from the load cells and chucks during stressing.

The final effective stresses on each connection were very close to the design values. The initial design stress for the system comprised of two strands per beam line was 164 psi and the measured stress after immediate losses was 167 psi. The initial stress for the system with four strands per beam line was designed as 328 psi and as-built stress was 340 psi. The actual values were slightly higher but reasonably close.

The VWGs in the second set of post-tensioned connections were monitored during construction and prior to the load tests. The strain ranges in the 340 psi stressed panels across all four VWGS were measured to observe strain changes prior to the cyclic testing of the deck. There were 53 days between making the deck composite and applying the first load test. Figure 38 shows the change in strain of the VWG on the exterior side of the post-tensioned connection. The other VWGs displayed similar trends.

The strands were stressed over a two-day period. The increase in strain in the concrete panels as measured by the embedded VWGs over this two-day period was $82.3 \mu\epsilon$. Based on the measured force applied and the modulus of elasticity calculated based on measured strength of the panels, the expected strain was $70.5 \mu\epsilon$. The difference between measured and predicted strain was 14%.

Table 9. Stress Levels in the Post-Tensioned – 340psi Specimen

	Final Force (kips)	Stress (ksi)	% f_{pu}
Strand 1	27.4	164	60.7
Strand 2	27.1	162	60.1
Strand 3	27.0	161	59.8
Strand 4	31.3	187	69.3
Strand 5	29.0	174	64.3
Strand 6	28.9	173	64.1
Strand 7	29.8	179	66.2
Strand 8	28.2	169	62.5
Slab	229	0.340	

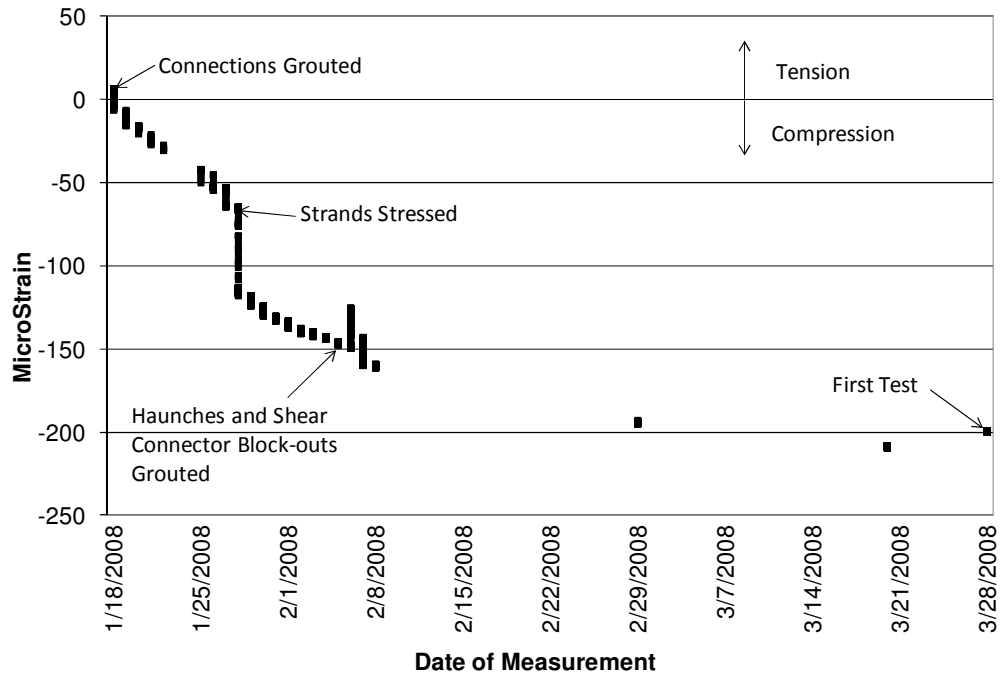


Figure 38. Panel Strain Prior to Testing for the 340 psi Post-Tensioned Specimen

By the end of grouting of the strands, VWG 1 read about $130 \mu\epsilon$ in compression. This continued to increase to about $150 \mu\epsilon$ in compression over the next eight days. On February 5th, the haunches and pockets were grouted. At this point the system was composite. After the last grouting procedure the specimen was monitored for 53 days prior to the initiation of testing. Over this period, the strain increased by about $50 \mu\epsilon$ at all VWGs. The final value in VWG1 was about $200 \mu\epsilon$ compression.

Cracking in the Panel-to-Panel Connections

The cracks in the deck were measured from the day after placing the grout to the end of the cyclical tests. The size and location of cracks were measured at key points in the test. This included cracks that appeared prior to loading, during the first load cycle, and at the end of the cyclical tests.

First Cracking

Shrinkage Cracks

The cyclical loading was started shortly after placing the grout in the deck panels. The time between the grouting of the transverse connections and the first loading was 7 days for the non-prestressed connections, 28 days for the 167-psi post-tensioned connection, and 71 days for the 340-psi post-tensioned connection. These times were not predetermined, but were the result of construction timing and lab accessibility. During these interim periods, the connections were visually monitored for cracking on the exterior surfaces.

The longer the connections sat before testing, the more the grout shrank. The first specimen with non-prestressed connections did not exhibit any visible cracks during the period before testing. It was monitored for only one week before testing began.

The first set of post-tensioned connections was monitored for 28 days prior to testing and had a few minor hairline cracks in the grout-only connection. The cracking occurred on the top surface of two of the post-tensioning duct-coupling block-out corners and on the overhang of the connection at the concrete-grout interface. The connection with pea gravel extension did not exhibit any initial cracking.

The last set of post-tensioned connections was monitored for over two months and cracked the most. The epoxy connection had a crack longitudinally through both of the post-tensioning duct-coupling block-outs on the top and bottom surface. There were also cracks on the bottom of the connection near the threaded rods used on the formwork. The normal grout had shrinkage cracks throughout the connection at the concrete-grout interface (Figures 39 and 40).

Shrinkage cracking was a problem in the panel-to-panel connection in these tests. The connections that cracked the most were the ones that were monitored the longest. The lack or presence of post-tensioning stress in the deck did not alleviate the problem. The connection with the highest compressive stress sat the longest and cracked the most.

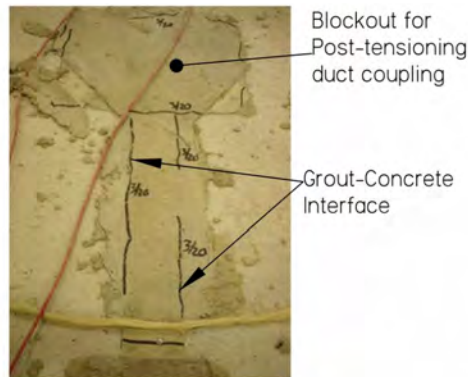


Figure 39. Shrinkage Cracks on Top of Deck in the 340 psi Post-Tensioned Connections

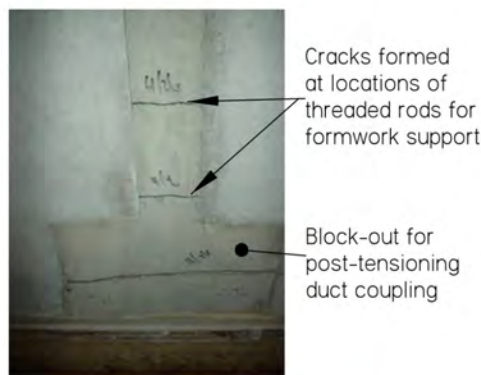


Figure 40. Shrinkage Cracks on Bottom of Deck in the 340 psi Post-Tensioned Connections

The First Load-Induced Cracks

During the first static load test, the panel-to-panel connections were carefully monitored for cracking. Visual observation and DEMEC readings were used to find the first crack. Graphs were made of the load versus strain recorded with the DEMEC points on the top surface of the panels. Table 10 presents the number of load cycles and load that caused the first crack in each connection.

The DEMEC data for the first load cycle for the looped bar connection are shown in Figure 41. Three measurements were made across this connection: one above each beam line and one at the midpoint between the beams. The exterior and interior lines on the graph indicate the two sides of the connection. The load versus strain diagram shows a large decrease in slope at the point of first crack. A clear change in slope is seen on the interior side of the connection at a load between 35 and 40 kips and on the exterior side at a load between 55 and 60 kips. The looped bar connection cracked at both concrete-grout interfaces during the first static load.

Table 10. Time and Load of the First Crack

Connection Name	First Cracking Load Based on DEMEC Data	Service Load Cycles at the First Crack
Looped Reinforcing Bars	35 kips	1
Drop-in Reinforcing Bars	55 kips	1
Post-Tensioned 167 psi Neat Grout	40 kips	1
Post-Tensioned 167 psi Pea Gravel Extended Grout	55 kips	1
Post-Tensioned 340 psi Neat Grout	70 kips	5000
Post-Tensioned 340 psi Neat Grout with Epoxied Faces	70 kips	5000

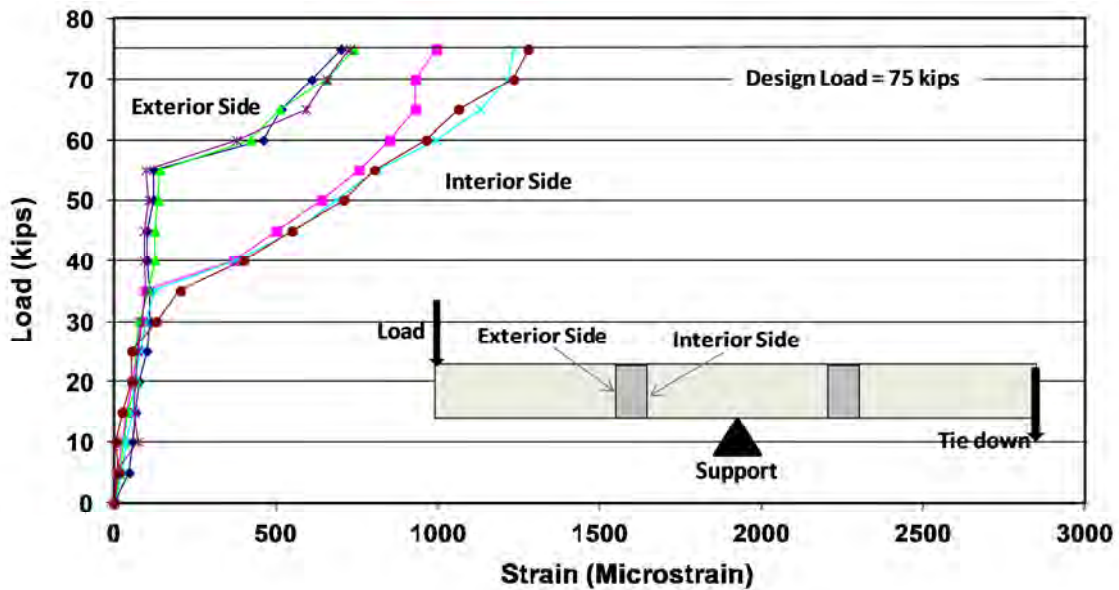


Figure 41. Load Versus Deck Surface Strain From DEMEC Points - Looped Reinforcing Bar Connection - One Service Load Cycle

The drop-in reinforcing bar connection cracked at approximately 55 kips on the first cycle (Figure 42). A large increase in strain from about $100\mu\epsilon$ to $1200\mu\epsilon$ is indicative of the appearance of the first crack. In addition the crack was visible during the initial load cycle. Both reinforced connections cracked prior to starting the cyclical load tests.

The four post-tensioned connections cracked at different loads and points in the cyclical loading. The initial cracks in the neat and extended grout connections with 167-psi level of stress occurred during the first static load (Figure 43). The neat grout connection cracked at 40 kips, whereas the extended grout cracked at 55 kips. In both connections, one transverse crack appeared on one side, at the grout-to-concrete interface, across the full width of the panels.

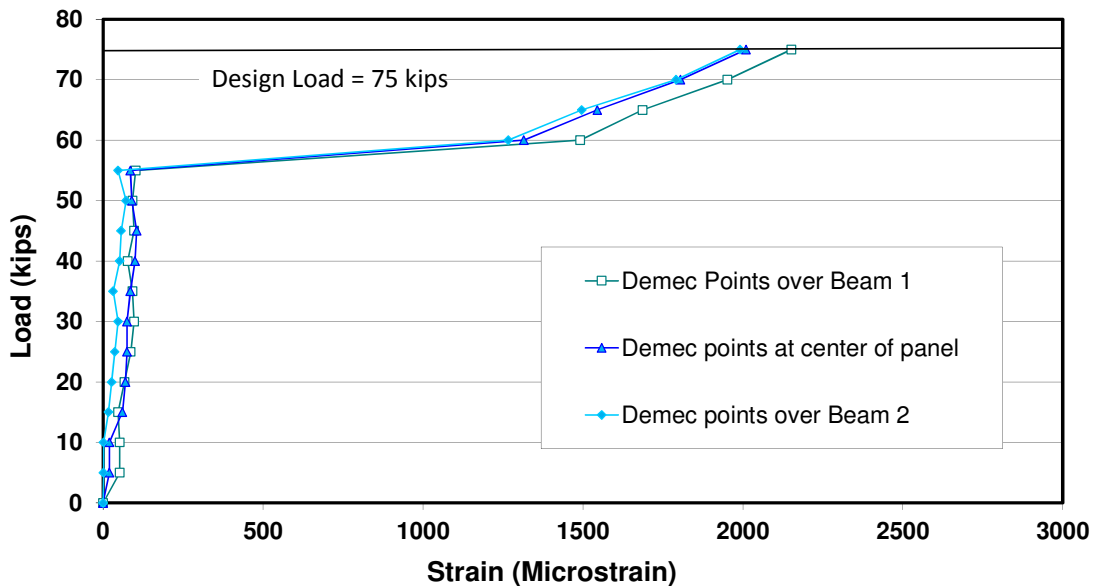


Figure 42. Load Versus Deck Surface Strain From DEMEC Points – Drop-in Reinforcing Bar Connection - One Service Load Cycle

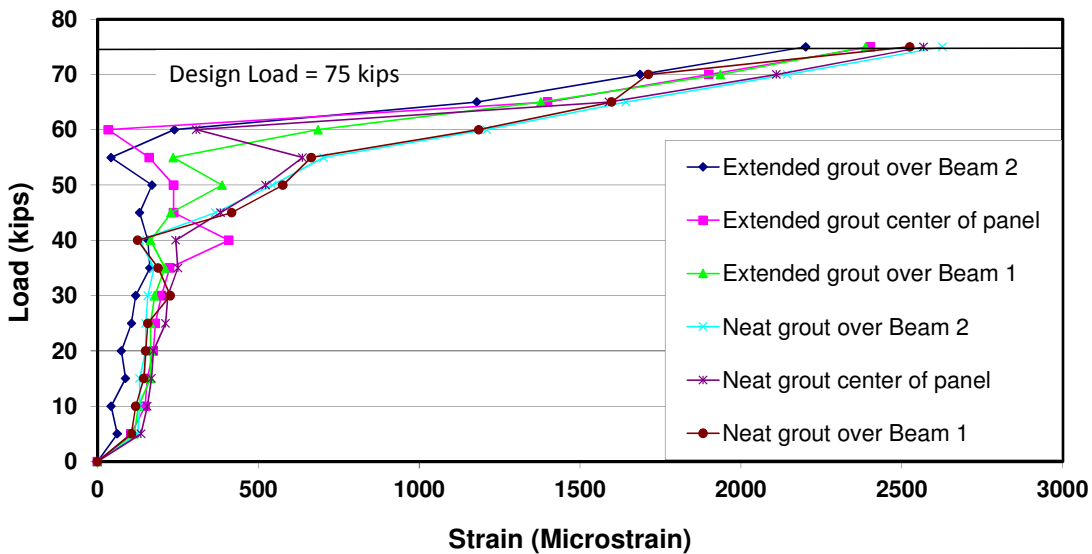


Figure 43. Load Versus Deck Surface Strain From DEMEC Points – Post-Tensioned Connections - 167 psi Stress – One Service Load Cycle

In the post-tensioned connections with prestress level of 340 psi, the connections did not experience large cracking. While no cracking was predicted, small shrinkage cracks occurred at the concrete-to-grout interface in the connections prior to service loading. The first crack due to service loads was seen at 5000 cycles for both connections; however, the DEMEC measurements on top of the deck were not conclusive (Figure 44). Figure 45 shows the load versus strain at 100,000 cycles with a slight nonlinearity. This nonlinearity in the graph never grew during the cyclical tests. The connection with the higher level of prestress did not exhibit large strains during any of the loadings as were seen in the previous four connections. Maximum surface strains in this connection peaked at about $800\mu\epsilon$, which is almost one-fourth the size of the maximum values in the other two post-tensioned connections. The cracks that did appear were extensions of the shrinkage cracks at the grout-to-concrete interface.

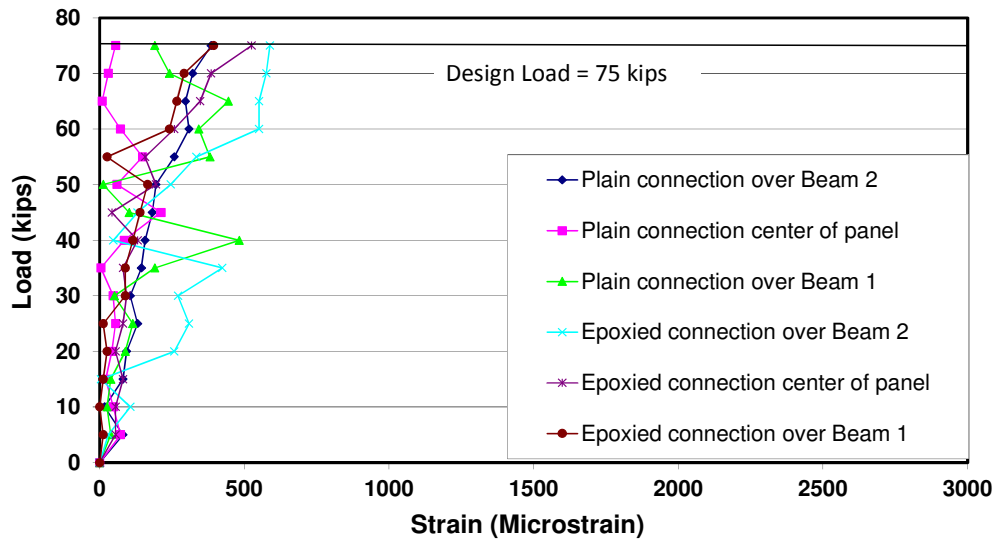


Figure 44. Load Versus Deck Surface Strain From DEMEC Points – Post-Tensioned Connections -340 psi Stress – One Service Load Cycle

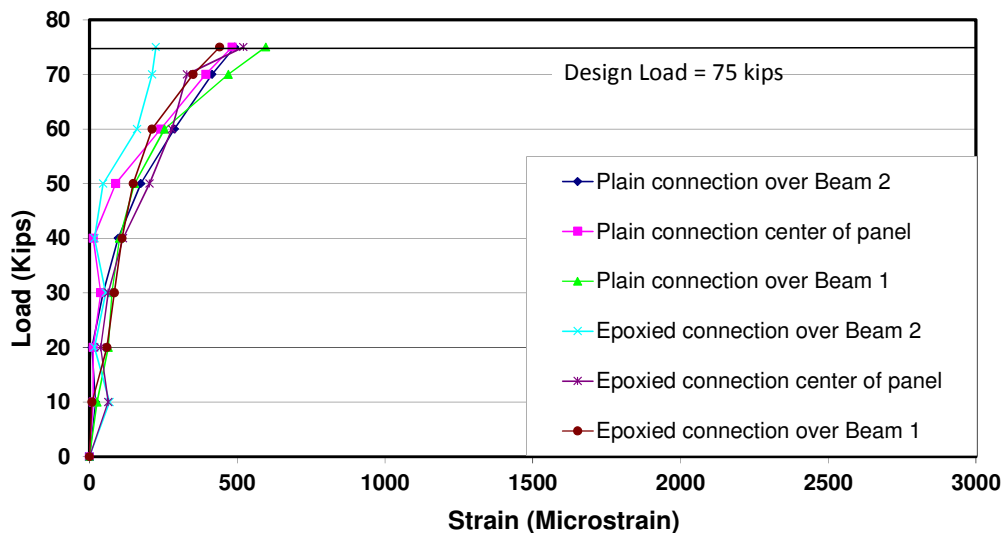


Figure 45. Load Versus Deck Surface Strain From DEMEC Points - Post-Tensioned Connections - 340 psi Stress – 100,000 Service Load Cycles

The first crack depended on the level of prestressing force. With little or no post-tensioning stress, the crack occurred on the first load cycle. When about twice the minimum prestressing force was applied, the first cracking occurred after a larger number of service load cycles and with a very minimal change in surface strain. A sufficient prestressing level postponed the first crack in the transverse connections and greatly reduced the strain gain after cracking.

Crack Expansion

The cyclical tests simulated the number of truck crossings expected on the Virginia bridge over 50 years. The cracking in the connection was carefully monitored at 100,000-cycle increments (10% of the total applied cycles of load) for crack propagation.

At the initial loading, the drop-in reinforcing bar connection cracked across the entire top and bottom surfaces of the concrete-to-grout interface at the exterior side of the connection. The vertical edge on each side of the transverse connection cracked at both the exterior and interior grout-concrete interfaces. The only major additional cracks occurred along the length of the drop-in bar cavities. Both exterior drop-in bar cavities cracked between 600,000 and 700,000 cycles (Figure 46). The cracks were formed primarily along the interface and not within the grout itself.

The looped bar connection had minor cracking throughout the connection. The cracking at the initial loading on both sides of the connection was not visible but did exist according to the strain measurements. Cracks became visible across the top of the connection on both sides of the grout-to-concrete interface around 20,000 cycles. There were no cracks visible on the bottom of the connection until 300,000 cycles. By 600,000 cycles there were cracks on the top and bottom surfaces of both sides of the connection. The cracks slowly became more visible along the entire connection. Additional cracking did occur longitudinally at 300,000 cycles along the connection where the tie rods were left in the grout (Figure 47). Otherwise, the cracks concentrated at the material interface. By the end of the cycles there was complete cracking along both interfaces.

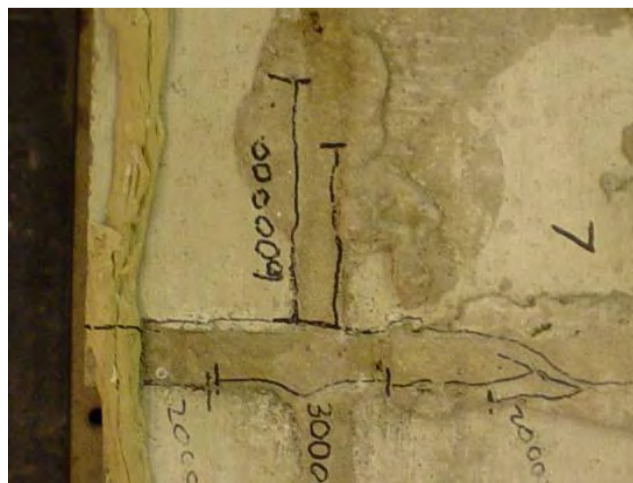


Figure 46. Cracks Along the Drop-in Bar Cavities on Top of Deck

The post-tensioned connection with 167-psi stress and pea gravel–extended grout had one full-width crack on the interior side of the grout-to-concrete interface at first loading. Over the course of the loading, the cracks did not change, but the area around the cracks developed spalling problems (Figure 48). The main crack went completely through the connection to the bottom of the panels and was visible on the vertical edges. Additional cracking appeared on the top and bottom of the deck around the block-out pockets where the post-tensioning duct was coupled. Most of the cracks occurred during the first static load cycle.

The 167-psi neat grout connection had one full-width crack on the exterior side of the connection and an additional crack along one half of the interior side of the connection. This crack on the interior extended to two-thirds of the grout-to-concrete interface before 200,000 cycles. The cracking extended to the bottom of the panels on the interior side of the connection. Cracking also appeared around the post-tensioning duct coupling block-out corners throughout the tests. More cracking appeared with the neat grout connection than with the pea gravel–extended grout connection.

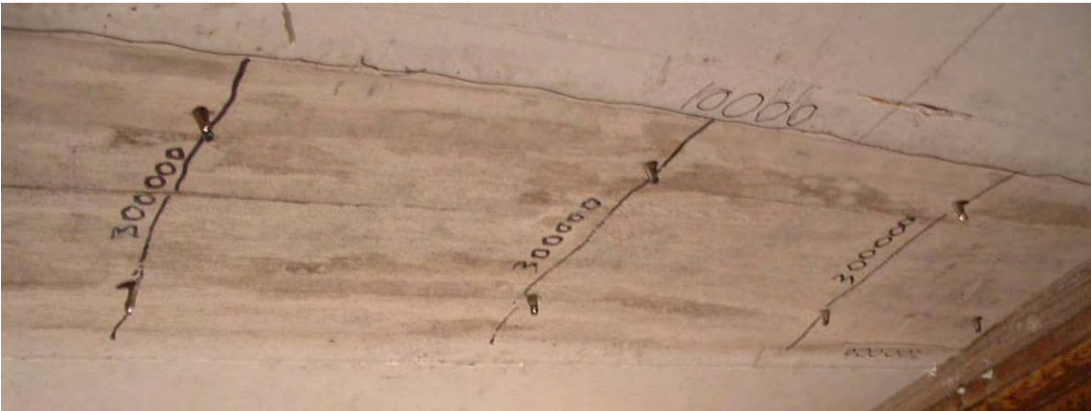


Figure 47. Longitudinal Cracking on the Bottom of the Looped Bar Connection

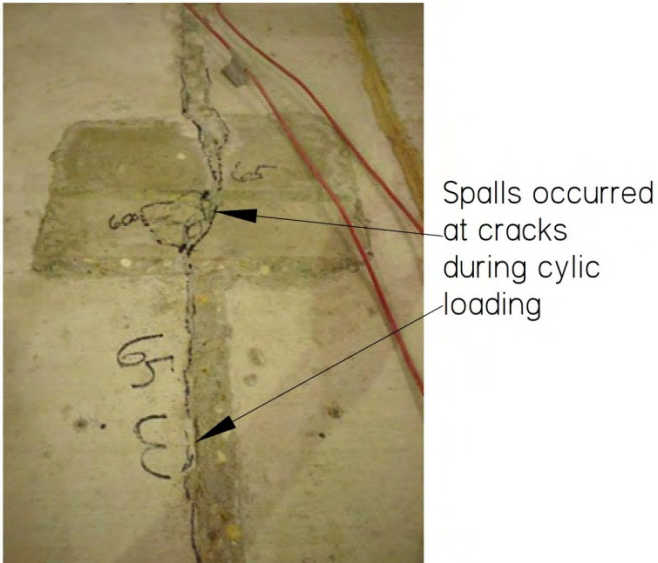


Figure 48. Spalling Along the Post-Tensioned Pea Gravel–Extended Grout Connection

The 340-psi post-tensioned connection with neat grout showed shrinkage cracking along most of the entire grout-to-concrete interface prior to testing. These cracks expanded throughout the load application (Figure 49). Vertical cracking on the edges of the panels and cracking on the bottom of the panels were never visible.

The 340-psi post-tensioned connection with neat grout and epoxy faces cracked in the middle of the block-outs for post-tensioning duct coupling prior to testing (Figure 50). During the first static tests a full-width crack appeared along the side of the connection closer to the support, which is the side with higher moment. Cracks occurred across the bottom of the connections at the threaded-rod locations. Shrinkage cracking expanded significantly around the corners and in the interior of the post-tensioning duct-coupling block-outs throughout the tests. There were never any visible cracks on the vertical sides or bottom of the panels.

In summary, the majority of the cracks occurred at the grout-to-concrete interface. The grout did not crack, except when epoxy was added to the material interface. Pea gravel caused spalling problems, but otherwise had similar crack patterns. Most of the cracks due to loading occurred during the first few thousand load cycles. Some extensions appeared after the initial loading, but very few new cracks appeared later in the tests of the post-tensioned connections. The cracks in the non-prestressed connections continued to widen until the end of the test.

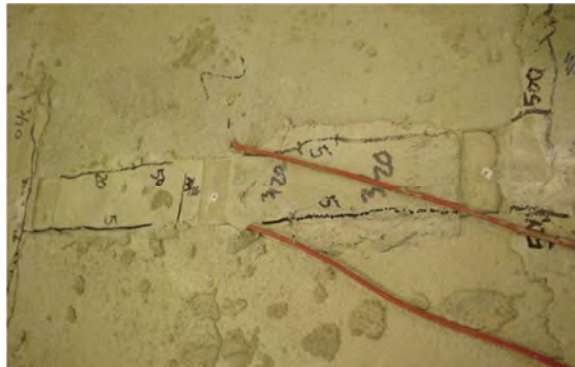


Figure 49. Surface Cracks in the Neat Grout 340 psi Transverse Connection (Note That Cracks Form on Both Sides of the Connection)

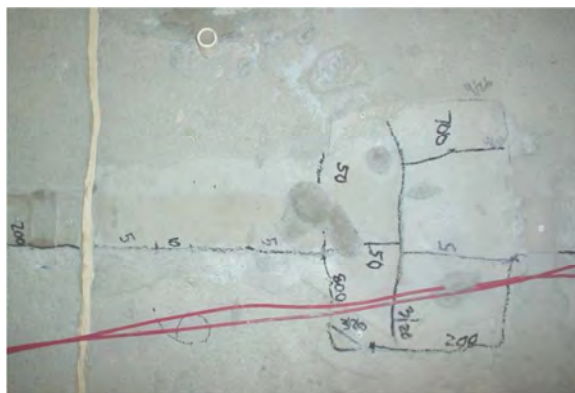


Figure 50. Cracks in the Neat Grout With Epoxy Faces, 340-psi Transverse Connection (Note Cracks Formed Along One Side of the Connection and Within the Post-Tensioning Duct Coupling Block-out)

Final Crack Widths

The location and width of the cracks were recorded at the end of the cyclical tests. The width of these cracks was measured with a crack gauge (0.005 in precision) on the top, side, and bottom surfaces of the transverse connections (Table 11). The crack distributions along the boundary interface and within the grout were recorded (Table 12). All of these values were measured with the service truck load applied (HS-20).

Three different types of grout material were used in the post-tensioned connections: grout extended with $\frac{3}{8}$ -in pea gravel, plain grout, and plain grout with an epoxy bonding agent applied to the surfaces. The extended grout cracked slightly less than the plain grout; however there were additional pop-out cracks on the top surface of the deck. The spalls may have been caused by the pea gravel in the extended grout. The epoxy bonding agent initially prevented shrinkage cracks at the concrete-grout interface. Once loading started, the epoxy connection cracked along the interface, but had fewer cracks in the block-outs for post-tensioning duct coupling. By the end of the tests the epoxy did not significantly alleviate cracking in the connections. Adding a pea gravel extension and epoxy did not significantly change the cracking width or patterns in the transverse connections.

The drop-in bar connection had the largest crack widths on both the top and bottom of the connection and the largest average crack width. The connections with 167 psi of post-tensioning stress had the second largest average crack width on the top. The looped bar connection cracks on the top were slightly larger than the average crack widths in the 340-psi post-tensioning connection. The connections with 340 psi of stress had the smallest cracks on the bottom of all the connections. In all cases, the post-tensioned connection with 340 psi of stress performed the best; however, the looped bar connection performed as well or better than the connections with 167 psi of stress. The benefit of the looped bar connection over the 167-psi stressed connections is that the cracks occurred over both interfaces, whereas the cracks in the post-tensioned connection occurred primarily on one side of the connection.

Records of bridge deck cracking in typical cast-in-place decks can be found in the literature. NCHRP Report 380 (Krauss and Rogalla, 1996) describes a cast-in-place deck on steel girders that had visible cracking after 18 days of air drying. The transverse cracking was found every 5 to 15 ft along the surface, with crack widths ranging from 0.005 in to 0.02 in. They did not report about leakage because the deck was placed on permanent metal deck forms. Extensive deck cracking, with crack widths in the range of 0.015 in to 0.06 in, were reported from the inspection of the Virginia Pilot Bridge of the Long Term Bridge Performance Program (Advitam, unpublished data). The through-cracks, which were full-depth and visible on the underside of the deck, showed evidence of water leakage and efflorescence. Corrosion on the top flanges of the steel girders was evident in the vicinity of the cracks. French et al. (2007) surveyed 38 bridge decks on steel girders and found 26 that had crack widths greater than 0.03 in. They noted in their surveys the leaking of through-cracks on decks with no permanent metal decks. Generally, typical cast-in-place bridge decks are prone to through-cracks due to restrained shrinkage, and research has been conducted to try to limit the cracking to the greatest extent possible.

Table 11. Final Surface Crack Widths in the Transverse Connections Measured at Service Load (in)

Location	Reinforcing Bar Connections		Post-Tensioned (PT) Connections			
	Looped Bars	Drop-in Bars	Pea Gravel Extended Grout (167 psi)	Neat Grout (167 psi)	Neat Grout (340 psi)	Neat Grout with Epoxy Faces (340 psi)
G2 Side Face	0.010	0.025	0.010	0.015	0	0
G2 Overhang Bottom	0	0.015	0	0.010	0	0
G1 Side Face	0.010	0.030	0.015	0.015	0	0
G1 Overhang Bottom	0.005	0.020	0.005	0.005	0	0
Top G1	0.015	0.025	0.015	0.015	0.010	0.010
Top Middle	0.010	0.025	0.015	0.015	0.010	0.010
Top G2	0.005	0.025	0.015	0.015	0.005	0.005
Bottom G1/PT Pocket	0.010	0.020	0.005	0.010	0	0.005
Bottom Middle	0.010	0.020	0.005	0.005	0	0
Bottom G2/PT Pocket	0.010	0.020	0.005	0.015	0.005	0.005
Average	0.010	0.025	0.010	0.010	0.005	0.005

Table 12. Final Crack Observations in the Transverse Connections

Location	Reinforcing Bar Connections		Post-Tensioned Connections			
	Looped Bars	Drop-in Bar	Pea Gravel Extended Grout (167 psi)	Neat Grout (167 psi)	Neat Grout (340 psi)	Neat Grout with Epoxy Faces (340 psi)
Top	Both sides of the connection cracked	One side completely cracked; the other was almost completely cracked	Almost all cracks on one side	Almost all cracks on one side	One main crack in middle; cracks surround edge of post-tensioning pocket	One main crack in middle; cracks surround edge of post-tensioning pocket
G1 Side (Elevation)	Both sides cracked	Both sides cracked	Inner side cracked	Outer side cracked; half of the inner side cracked	Horizontal cracks near shear keys	Horizontal cracks near shear keys
G2 Side (Elevation)	Both sides cracked	Both sides cracked	Inner side cracked	Outer side cracked	Horizontal cracks near shear keys	Horizontal cracks near shear keys
Bottom	Both sides cracked	Outer side cracked	One crack in the middle, cracks on the corner of the post-tensioning connection; crack between post-tensioning connections-inside only	One crack in the middle, cracks on the corner of the post-tensioning connections; crack between post-tensioning connection -inside only	A few slight cracks around post-tensioning pocket, perpendicular cracks to tie rods for formwork	Slight cracks around PT pocket; large longitudinal crack down middle of post-tensioning pocket, perpendicular cracks to tie rods for formwork

Ponding on the Deck Panels

Static ponding tests were performed on the surface of the decks to determine if cracking was large enough to allow water to flow through the deck. The tests were performed on the panels and connections while they had no service load applied, after increments of cyclic loading as noted in Table 2. Tap water was placed to a level of ¼ in within the containment area on the deck and left in place for two hours (Figure 22). The sides and bottom of the deck were monitored for water leakage through the connections.

The reinforced connections were tested first. Neither connection leaked for the first 500,000 cycles (Table 13). After 500,000-cycles, the drop-in bar connection began to leak along its entire length. The leaks started within 15 minutes of applying the water and continued for the duration of the test. The looped bar connection did not have any leaking at the same point in the test.

Table 13. Ponding Test Results as Measured by Visual Detection: Reinforcing Bar Connections

Stage of Loading	Reinforcing Bar Connections	
	Looped Bars	Drop-in Bar
500,000 Cycles	No Leaks	Leaks throughout
1,000,000 Cycles	No Leaks	Leaks throughout
10 Cycles with Water	25% of Interface Leaked	100% of Interface Leaked
100 Cycles with Water	75% of Interface Leaked	100% of Interface Leaked
Notes:	A small amount of water wetted most of the area beneath the looped bar connection.	The drop-in bar connection streamed water during the final ponding with load cycles.

At the end of the test, the looped bar connections did not leak and the drop-in bar connections leaked profusely. After the final static ponding test was performed, the test was repeated with 10 load cycles and with 100 load cycles applied during ponding. The cycles consisted of applying the equivalent of HS-20 service load at 1 Hz. While under the cyclic load and ponding, the drop-in bar connection leaked profusely. Water continuously flowed through the cracks in the middle of the connection. Approximately 25% of the looped bar connection began to leak under the 10-cycle load. By the end of 100 cycles under ponding, about 75% of the looped bar connection showed signs of leaks (Figure 51). Most of the water beaded up along the crack between the grout and concrete but did not drip to the ground.

The first post-tensioned specimen had two connections with 167 psi of initial compressive prestress: One connection with neat grout and one with a pea gravel–extended grout. Neither connection leaked until the static test after one million cycles. During this test, the pea gravel connection had three small leaks between the grout and panels that were 1 to 2 in long (Table 14). There was no significant change in the pea gravel connection until ponding with 100 cycles of service load. At the conclusion of the 100 cycles, approximately two-thirds of the connection leaked (Figure 52). Water beaded up on the cracks between the grout and panels but very little water leaked to the ground.



a) Looped Bar Connection

b) Drop-in Bar Connection

Figure 51. Final Leaking - Reinforced Concrete Connections

Table 14. Ponding Test Results as Measured by Visual Detection: Post-Tensioned Connections

Stage of Loading	Post-Tensioned (PT) Connections			
	Pea Gravel-Extended Grout (167 psi)	Neat Grout (167 psi)	Neat Grout (340 psi)	Neat Grout with Epoxy Faces (340 psi)
500,000 Cycles	No Leaks	No Leaks	No Leaks	No Leaks
1,000,000 Cycles	3 Leaks – 1 to 2 in long	1 Leak – PT Pocket 1 in long	No Leaks	No Leaks
10 Cycles with Water	3 Leaks – 1 to 2 in long	1 Leak – PT Pocket 1 in long	No Leaks	No Leaks
100 Cycles with Water	~66% of Interface Leaked	~20% of Interface Leaked	No Leaks	No Leaks



a) Pea Gravel Extended Grout



b) Neat Grout

Figure 52. Final Leaking - Post-Tensioned Connections With 167-psi Prestress

The neat grout connection had one minor crack on the corner of one of the duct-coupling block-outs that leaked water. The leaking portion of crack was approximately 1 in long. This connection leaked very little and did not have water beading up around it until the conclusion of the test. After the 100 cycles with the water, about twenty percent of the connection between the panels leaked water. The water beaded up in a few spots and did not drip to the ground. There was less water moving through this connection as compared to the pea gravel connection.

The last specimen had two post-tensioned connections with 340 psi of compressive prestress. Both connections were identical except for an epoxy bonding agent between the grout and panel interface on one connection. Neither leaked water at any of the interface cracks during the static ponding tests or the ponding tests with cyclical loads.

The post-tensioned connections with the highest level of post-tensioning exhibited the best behavior in the ponding tests and had the smallest cracks. Connections with average crack sizes of 0.005 in or less never leaked. The looped reinforcing bar connection also exhibited satisfactory results, although it did leak a minor amount at the end of the testing. Connections with average crack sizes of 0.010 in or greater leaked by the end of cyclic loading. The connections with the lower level of prestressing and the drop-in bar connections performed the worst. They would not be recommended based on the ponding results.

Load-Strain Profiles in the Panel-to-Panel Connections

The strain profiles were determined based on the measurements from electrical resistance strain gages on the beams and VWGs inside the concrete panels. Profiles were developed for each static load test. The theoretical strain distribution was computed using the service load moments and the uncracked transformed section properties for the prestressed cross-sections and also with the cracked transformed section properties for the two non-prestressed connections. The material properties determined from tests of companion cylinders were used for the concrete (f'_c and E_c) along with the assumed properties for steel (E_s). Full composite action between the deck and beam was assumed for all models.

Figures 53 through 55 show the strain profiles at each connection at two load levels (40 kips and 75 kips) that were recorded during the static load tests performed after 1,000,000 cycles of load had been completed. The calculated strain profiles at the service load level, 75 kips, is shown. As can be seen in Figure 53, the non-prestressed connections exhibited non-linear strain distribution. The cracking at the connection prevented the concrete adjacent to the VWG from developing significant tensile stresses and strains, so the strain remains near zero throughout loading. The neutral axis location was somewhat higher than predicted with the cracked transformed section analysis.

Figures 54 and 55 present the strain profiles for the post-tensioned connections. All indicate that some cracking had occurred, but the performance of the more highly prestressed (340 psi) connections was better. The strain distribution was closer to linear, and the neutral axis location was higher in the cross-section.

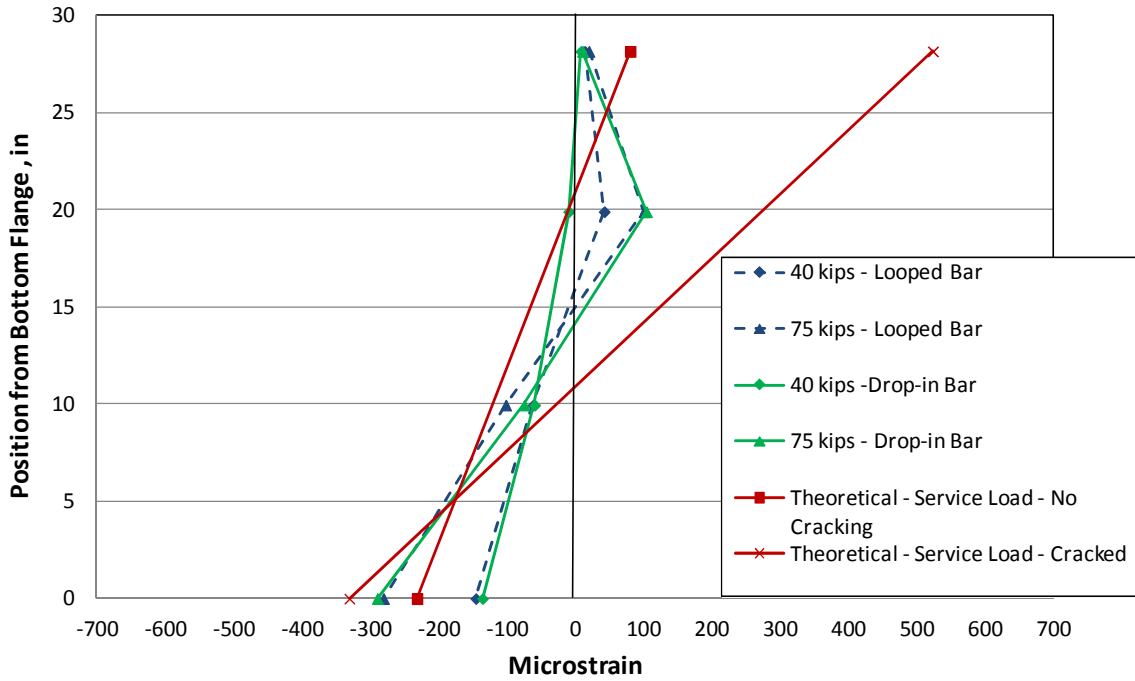


Figure 53. Strain Profile for the Non-Prestressed Connections

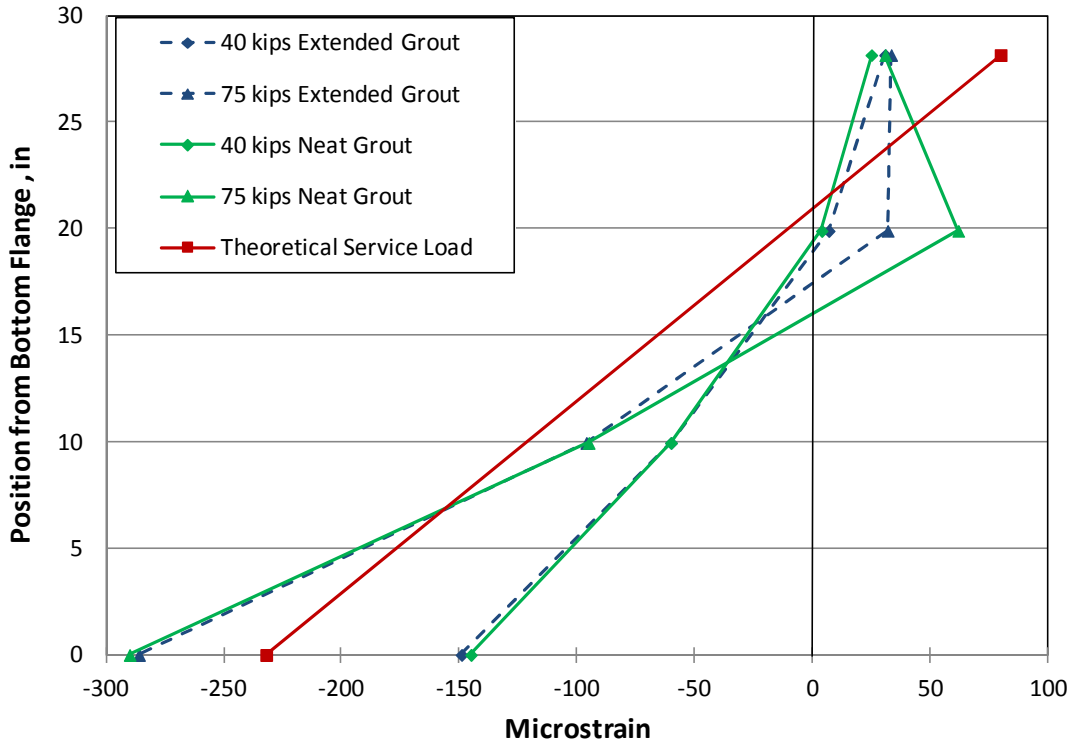


Figure 54. Strain Profile for 167-psi Post-Tensioned Connections

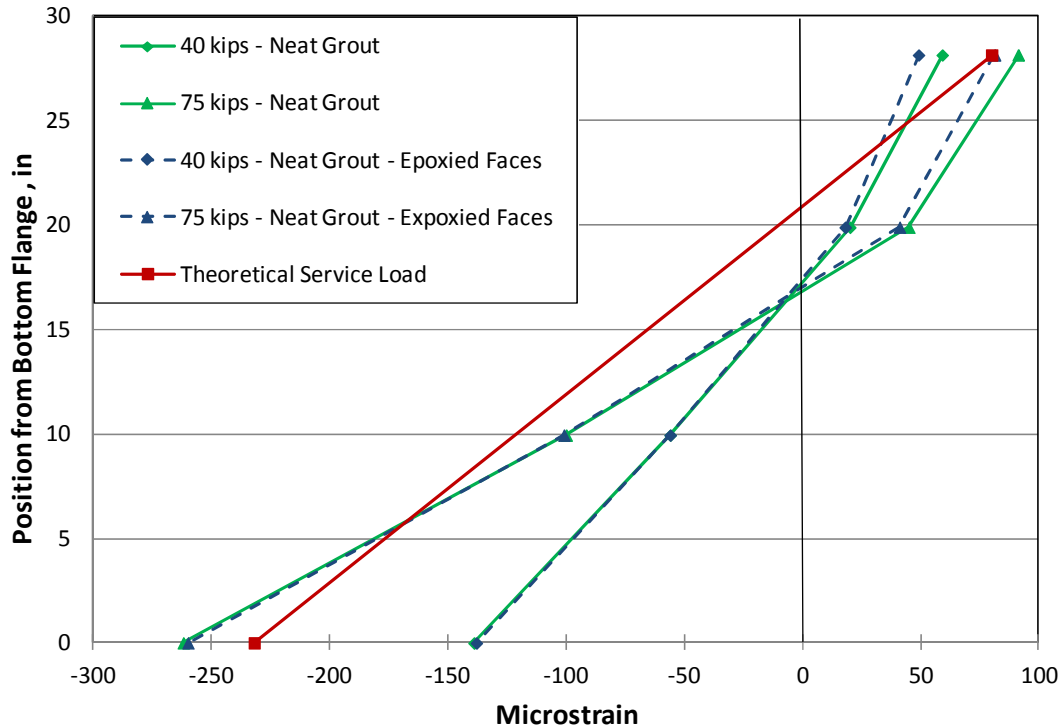


Figure 55. Strain Profile for 340-psi Post-Tensioned Connections

At all connections subjected to the 75 kips load, the neutral axis location was lower in the cross-section than was predicted using the uncracked transformed section analysis. The neutral axis moved down towards the mid-height of the steel beam (10.7 in) as the deck redistributed strain to the beams. For the connections with 340 psi of prestress, the neutral axis consistently stayed around 17 to 18 in from the bottom flange in the beam web. In the 167-psi prestressed connections, the neutral axis moved to about 16 to 17 in from the bottom flange. In the looped reinforced connections, the neutral axis dropped to about 15 in from the bottom flange. The drop-in bar connection's neutral axis dropped to about 14 in from the bottom flange. The 340-psi post-tensioned connections had the highest neutral axis of all the connection types.

Cracking was observed in all of the transverse connections to some degree. The cracks were primarily parallel to the panel face at the grout-to-concrete interface. These cracks indicated that there was a loss in compression in the concrete deck panels. The lower neutral axis positions were likely due to the effects of cracking.

Load Versus Strain in the Transverse Connections

The strains in the transverse connections were measured using VWGs in the concrete panels. One VWG was placed on each side of the connection. The VWGs were placed at the longitudinal centerline of the panel in the post-tensioned connections. The VWGs were positioned approximately midway between the reinforcing bars in the drop-in bar and looped bar connections (Figure 56). Additionally, the surface strain across the connections was measured using DEMEC points (Figure 57). The readings from these devices provided an indication of how much strain the top surface of the panels underwent during service loading over time.

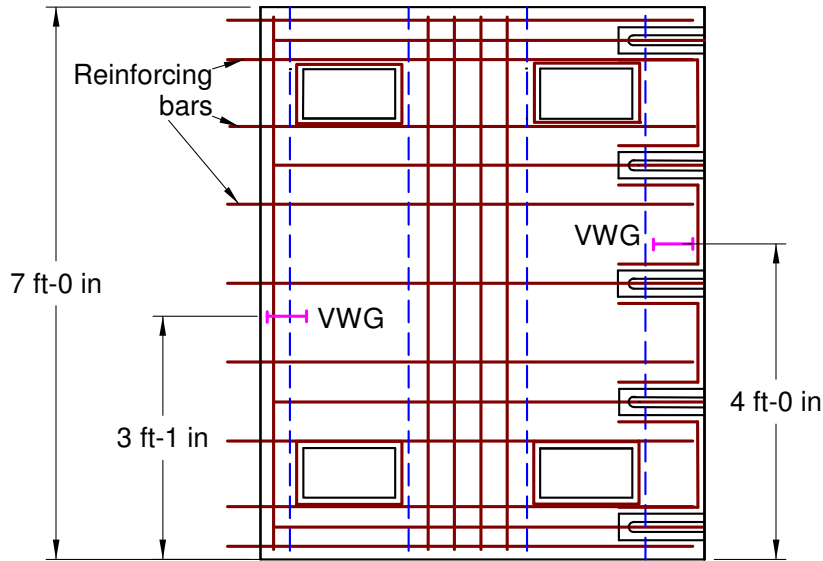


Figure 56. VWG Location on a Plan View of the Drop-in and Looped Bar Connections

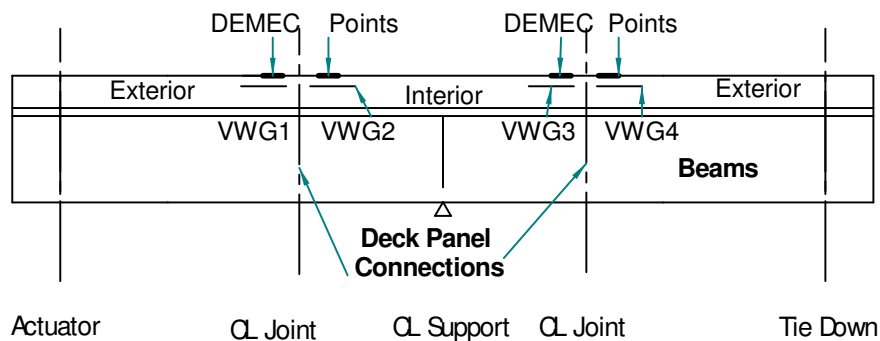


Figure 57. VWG Locations

As discussed previously, DEMEC strain readings and Vibrating Wire Gage (VWG) strain readings were used to determine the load stage at which the load-versus-strain behavior first deviated from linear. This was considered the first cracking load.

The DEMEC points were read at 5-kip intervals during the initial static loading, and at 10-kip intervals during static loading performed at stages during cyclic testing. Plots of load versus strain were created and Figure 58 presents the plots for the first static load test. The strains presented are the average of the three DEMEC readings across each connection. All connections initially exhibited linear load-versus-strain behavior, and four connections had a distinct load at which the slope of the line decreased dramatically. This point was selected as the first cracking load, and the cracking loads for each connection are presented in Table 15. The more highly stressed post-tensioned connections did not exhibit non-linear load-versus-strain behavior until after 5000 cycles of load, at 70 kips of applied load.

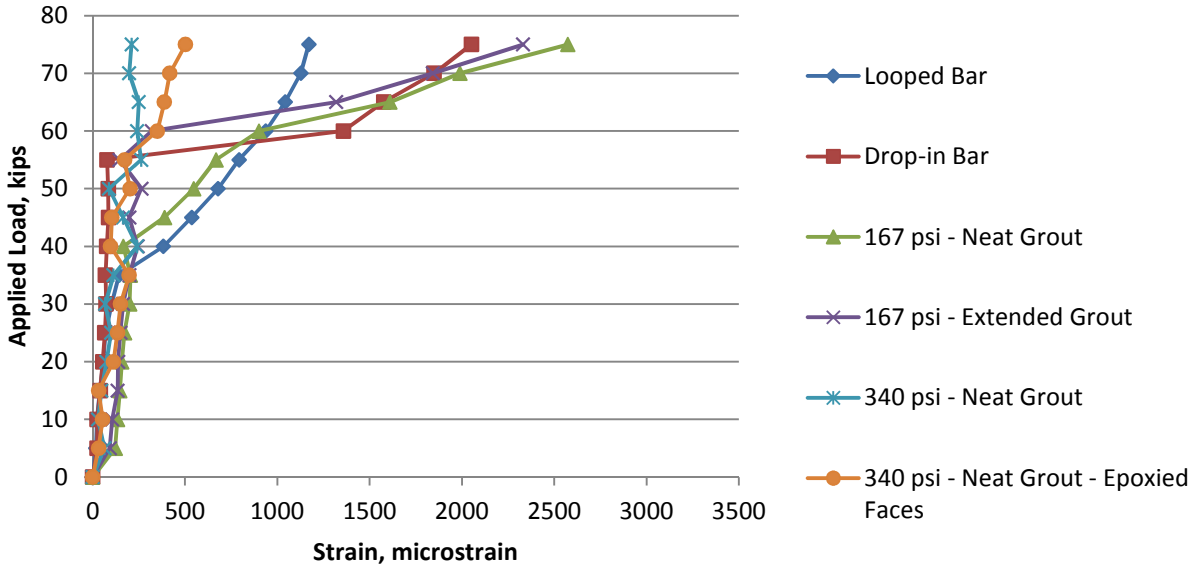


Figure 58. Plot of Load Versus Strain from DEMEC Gages on First Load Cycle

Vibrating wire gage readings were collected every thirty seconds during each static load test. At each load interval, the load was held constant long enough for at least two readings of the VWGs. The plots of VWG strain versus load are presented in Figure 59. Before cracking the strains increase linearly with applied load. Because the VWGs are immediately adjacent to the crack, but do not cross it, after cracking the level of strain in the gages does not continue to increase at the same rate. This is because there can be no increase in tension across the open crack. So, based on the load versus strain plots, the cracking load was taken as the load at which the slope of the line distinctly increases. These loads are presented in Table 15.

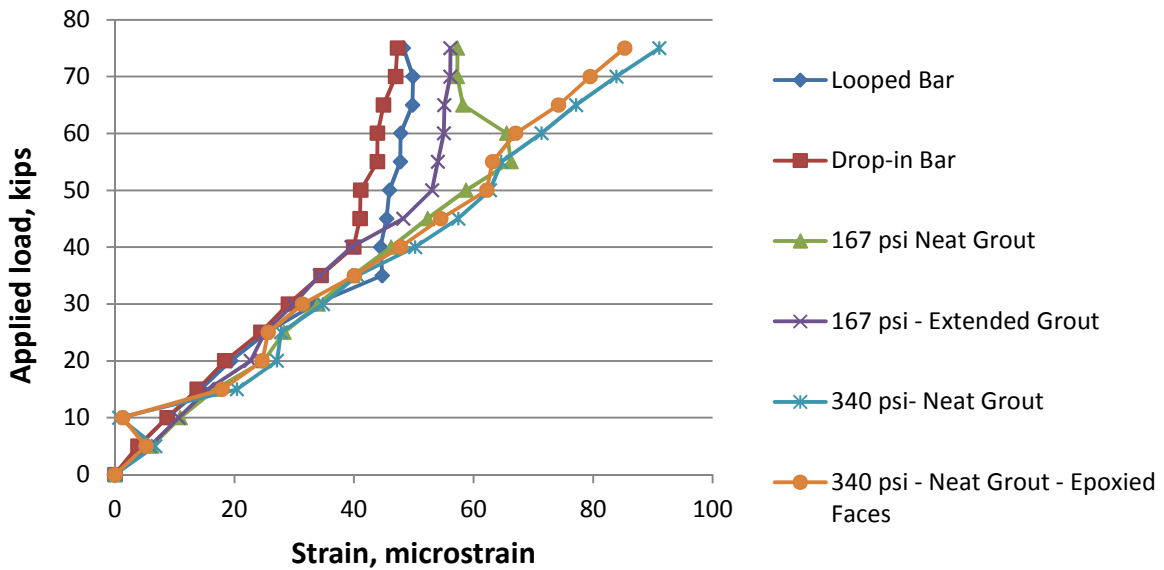


Figure 59. Plot of Load Versus Strain From VWGs on First Load Cycle

Table 15. First Cracking Loads and Stresses

Connection	DEMEC First Cracking Load, kips	VWG First Cracking Load, kips	Service Load Cycles at the First Crack	DEMEC Applied First Cracking Stress, psi	VWG Applied First Cracking Stress, psi	Initial Pre-Compression, psi	DEMEC Net Cracking Stress, psi	VWG Net Cracking Stress, psi
Looped Reinforcing Bars	35	35	1	273	273	0	273	273
Drop-in Reinforcing Bars	55	40	1	400	292	0	400	292
Post-Tensioned 167 psi, Neat Grout	40	55	1	292	401	167	125	234
Post-Tensioned 167 psi, Extended Grout	55	50	1	401	364	167	234	197
Post-Tensioned 340 psi, Neat Grout	70	70	5000	510	510	340	170	170
Post-Tensioned 340 ksi, Neat Grout-Epoxy	70	70	5000	510	510	340	170	170

Table 16 presents the cracking stresses compared to the compressive strength of the grout in the connections. The stress in the connection at the first cracking load varied between $1.9\sqrt{f'_c}$ and $5.9\sqrt{f'_c}$, with an average based on both strain measurements of $3.3\sqrt{f'_c}$.

Figures 60 and 61 present the load versus strain data based on DEMEC gages and VWGs during the static load test performed after 1,000,000 cycles. The post-tensioned connections with 340-psi pre-compression performed the best based on both types of strain measurements, with the plot remaining linear to a significantly higher load than the other connections. Also the maximum strain at service load (75 kips) as measured with the DEMEC gages, which crossed the connections, was the smallest for the highly pre-compressed connections.

Table 16. Cracking Stresses Relative to Grout Compressive Strength

Connection	DEMEC Net Cracking Stress, psi	VWG Net Cracking Stress, psi	Grout Compressive Strength, f'_c , psi	DEMEC Net Cracking Stress/ $\sqrt{f'_c}$	VWG Net Cracking Stress/ $\sqrt{f'_c}$
Looped Reinforcing Bars	273	273	4640	4.0	4.0
Drop-in Reinforcing Bars	400	292	4640	5.9	4.3
Post-Tensioned 167 psi, Neat Grout	125	234	3970	1.9	3.7
Post-Tensioned 167 psi, Extended Grout	234	197	4700	3.4	2.8
Post-Tensioned 340 psi, Neat Grout	170	170	5360	2.3	2.3
Post-Tensioned 340 psi, Neat Grout – Epoxy Faces	170	170	5360	2.3	2.3

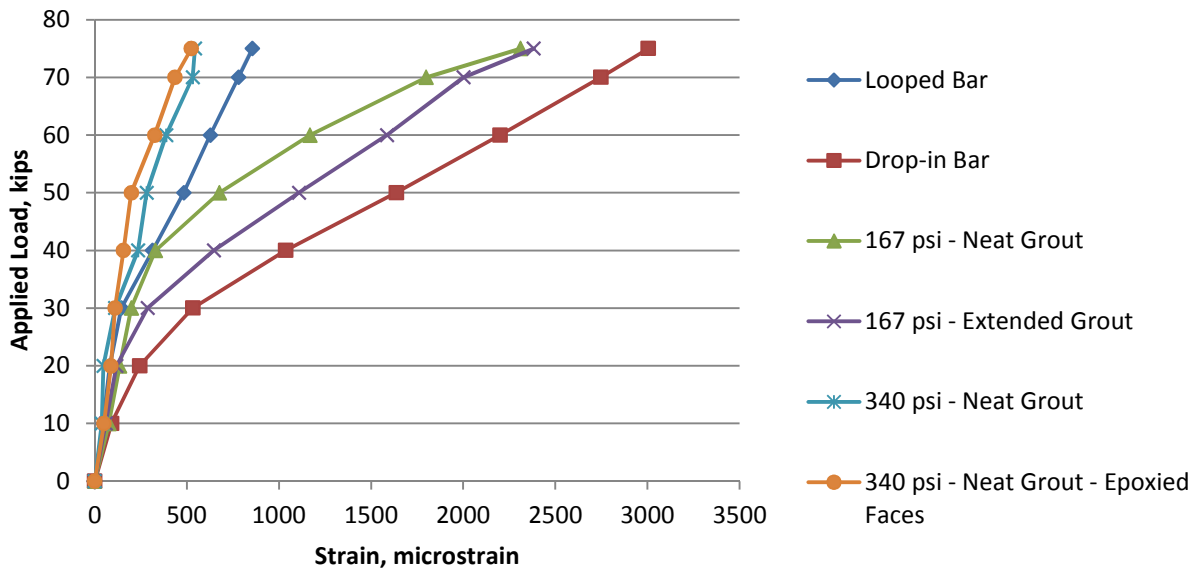


Figure 60. Plot of Load Versus Strain From DEMEC Gages After 1,000,000 Cycles

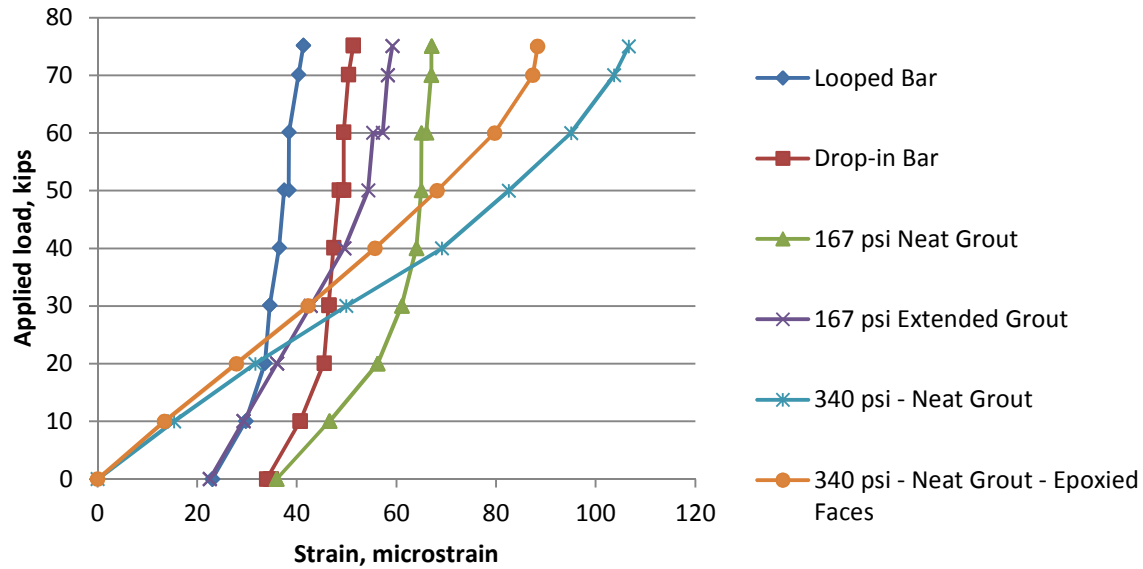


Figure 61. Plot of Load Versus Strain From VWGs After 1,000,000 Cycles

Comparison of Stress Levels, Cracking, and Leaking

One of the objectives of this research is to recommend a level of prestress that will result in durable panel-to-panel connections. Table 17 presents the maximum net stress applied during cyclic loading (stress due to applied load minus pre-compression), how this stress compares to the square root of the compressive strength of the grout, the resulting average crack width, and whether the connections leaked while subjected to loading cycles. For these specimens, 340 psi of compression kept the net stress below $3\sqrt{f'_c}$, which kept the average crack width below 0.005 in. Cracks this small did not leak. AASHTO LRFD (2012) Table 5.9.4.2.2-1 sets the maximum tensile stress at service limit state for components that are subjected to severe corrosive conditions at $3\sqrt{f'_c}$. Therefore, limiting the net stress at panel-to-panel connections to $3\sqrt{f'_c}$ is consistent with AASHTO's recommended stress level for a deck exposed to deicing chemicals.

AASHTO LRFD (2012) does not explicitly limit crack widths, however in commentary section C5.7.3.4, a crack width of 0.013 in is presented as the basis of the spacing requirement to control cracking in exposure conditions where there is an increased concern for corrosion. Eurocode 2 (BS EN 2004) has the identical requirement of 0.013 in for exposure condition XD3, which includes bridge decks. ACI Committee 224 (ACI 224, 2008) has somewhat stricter recommendations, with 0.007 in suggested as a reasonable crack width with exposure to deicing chemicals and 0.004 in for water retaining structures. Based on these references, all connections except the drop in bars had crack widths that would be deemed acceptable in a bridge deck environment. However, only the highly post-tensioned connections, which had maximum crack widths of 0.005 in, will minimize the possibility of leakage.

Table 17. Final Surface Crack Sizes Under Service Loads

	Non-Prestressed Connections		Post-Tensioned Connections			
	Looped Bars	Drop-in Bars	167 psi Extended Grout	167 psi Neat Grout	340 psi Neat Grout	340 psi Neat Grout with Epoxy
Maximum Net Stress During Cycling, psi	540	540	370	370	200	200
Maximum Relative to f'_c	$7.9\sqrt{f'_c}$	$7.9\sqrt{f'_c}$	$5.4\sqrt{f'_c}$	$5.9\sqrt{f'_c}$	$2.7\sqrt{f'_c}$	$2.7\sqrt{f'_c}$
Average Final Crack Size, in	0.010	0.025	0.010	0.010	0.005	0.005
% of Interface with Leaks Under Load	75%	100%	66%	20%	No Leaks	No Leaks

Strain Increases With Cyclic Loading

Table 18 presents the maximum strains measured with the DEMEC gage for each connection at the first cycle and the cycle that exhibited the largest strain. The drop-in bar connection had the largest strain increase during cyclic testing.

Table 18. Average Range of Strain in Each Connection

Connection	First Cycle Maximum Strain ($\mu\epsilon$)	Largest Maximum Strain ($\mu\epsilon$)	Number of Cycles at the Maximum Strain
Looped Reinforcing Bars	1714	1714	0
Drop-in Reinforcing Bars	2051	3004	1,000,000
Post-tensioned 167 psi – Neat Grout	2573	2612	1000
Post-tensioned 167 psi - Pea Gravel Grout	2330	2491	800,000
Post-tensioned 340 psi – Neat Grout	210	690	700,000
Post-tensioned 340 psi – Neat Grout with Epoxy Faces	502	533	900,000

Deflection of the Cantilevered Test

During each static load test, the maximum vertical deflection of the beams was measured directly beneath the loaded end of the cantilever test. A comparison was made of the maximum deflections versus the number of load cycles for each test setup. Table 19 shows the deflection at key points throughout the tests. Figure 62 through Figure 64 show the progression of deflections during the tests.

Table 19. Maximum Deflections of the Transverse Connection Tests

Cycles	Maximum Deflections (in)		
	Reinforcing Bars	Post-Tensioned 167 psi	Post-Tensioned 340 psi
1	0.464	0.420	0.386
10,000	0.425	0.394	0.384
20,000	0.397	0.394	0.399
100,000	0.419	0.394	0.399
500,000	0.417	0.405	0.409

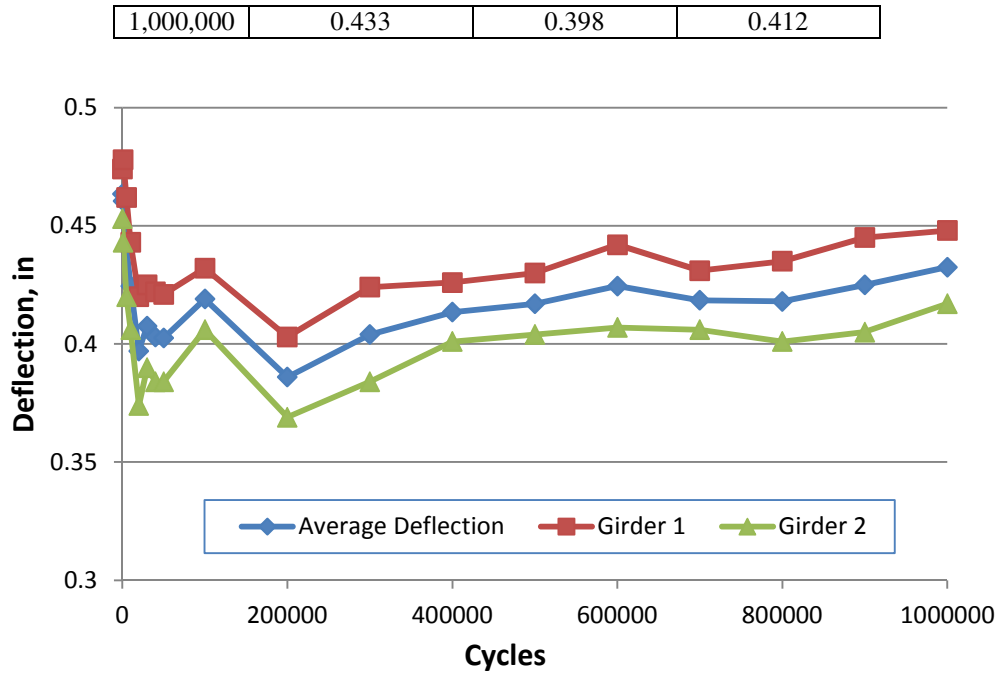


Figure 62. Maximum Deflection of the Beams Versus Load Cycles – Non-Prestressed Connections

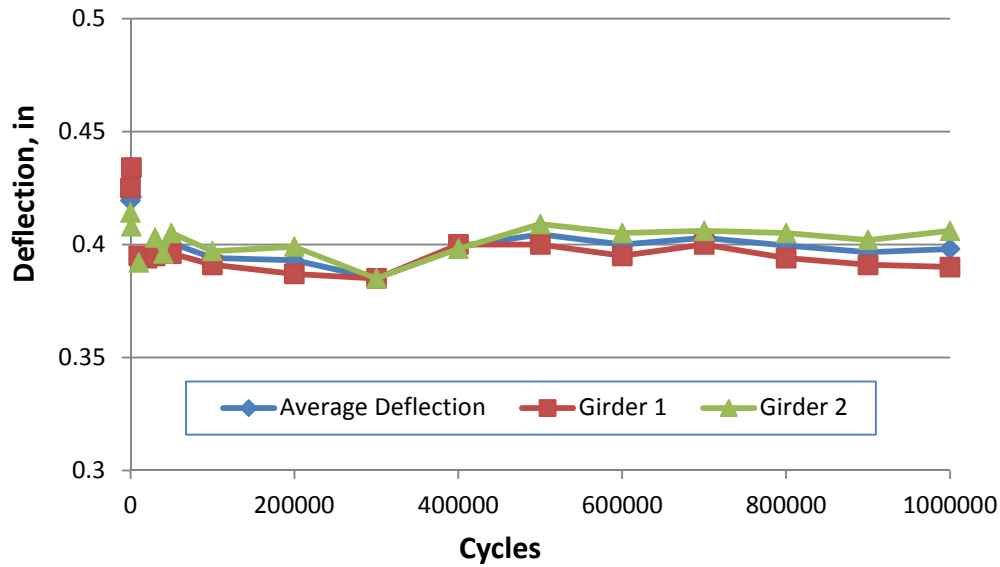


Figure 63. Maximum Deflection of the Beams Versus Load Cycles – 167 psi Post-Tensioned Connections

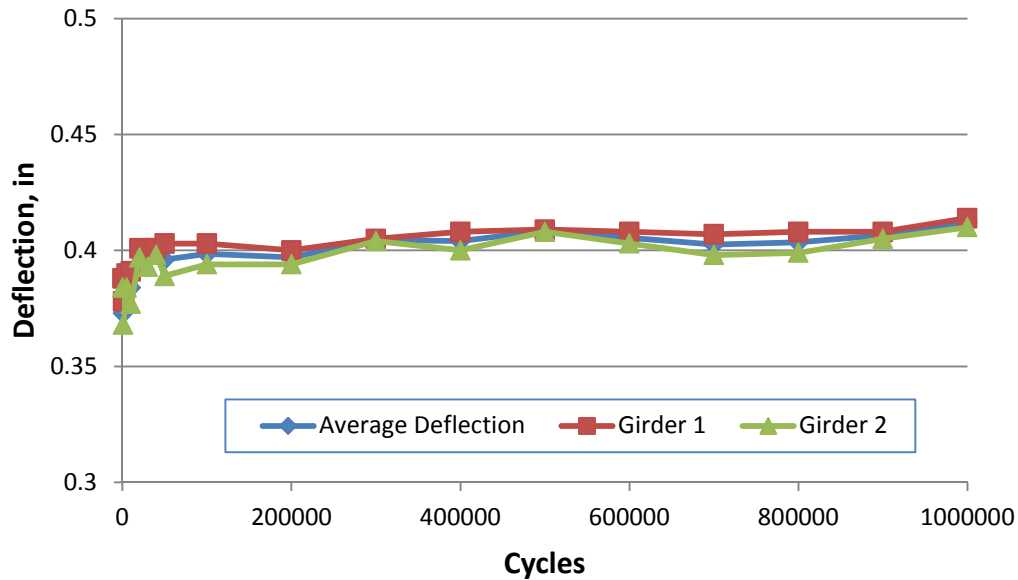


Figure 64. Maximum Deflection of the Beams Versus Load Cycles – 340 psi Post-Tensioned Connections

The deflections of the non-prestressed system dropped during the first 10,000 cycles, due to tightening of the tie-down points in the system. After the effect of the tightening was discovered, the bolts were not adjusted for the remainder of cycling. From 20,000 cycles through the end of the test, the deflections slowly increased. The average maximum deflection of the beams at 20,000 cycles was 0.397 in. The deflection slowly increased and peaked at 0.433 in at the end of the test. The deflection increased 9.0% from 20,000 through 1,000,000 cycles.

The system with post-tensioned connections with 167 psi of effective prestress dropped in deflection initially. This was also due to tightening the tie-down points during the first 10,000 cycles. By 10,000 cycles, the system stabilized at a maximum deflection of 0.394 in. The values increase to 0.405 in at 500,000 cycles before finishing at a value of 0.398 in. The maximum percent increase in deflection was 2.8%; however, the final percent difference was 1.0%.

The post-tensioned connections with 340 psi of effective prestress initially increased in deflection. Unlike the previous two tests, the tie-down was not tightened during the first 10,000 cycles. The previous two systems began with abrupt changes in deflection because the systems settled in place; therefore, the deflections that occurred after 10,000 cycles were used for comparison in this system. By 20,000 cycles, the system stabilized at a maximum deflection of 0.399 in. The values increase to 0.412 in by the end of the test. This corresponded to a maximum percent increase in deflection of 3.3%.

The post-tensioned systems increased in deflection the least throughout the tests. The 167-psi system increased in deflection 2.8% while the 340-psi system increased in deflection by 3.3%. When looking at the graphs in Figures 63 and 64, the change in deflection over time is barely detectable.

Shear Pocket Surface Treatment Results

Transverse panel-to-panel connections, shear pockets, and post-tensioned block-outs are filled with grout on precast full-depth deck panels. In the first two sets of transverse connection tests, extensive cracking was observed around the shear pockets. In the second post-tensioned transverse connection test, a variety of strategies were used to attempt to prevent cracking.

Grout Observations on the First Two Transverse Connection Specimens

On the first two transverse connection specimens, a highway patch grout was used on all the transverse connections, shear pockets, and haunches. This grout was chosen because the producer sells it as a low shrinkage, high early strength grout and it had performed satisfactorily in previous tests (Scholz et al 2007). During the tests, observations were made of all cracking that occurred on the surfaces of the panels. This included close inspection of the shear pockets.

As discussed in the METHODS section of this report, each transverse connection specimen had twelve shear pockets. Each of the three panels in a specimen had four pockets (Figure 64). Inside each pocket, eight shear studs were welded to the steel beam beneath the panels. The pockets were filled with high early strength, low shrinkage grout to make the system composite.

The first specimen was built with two reinforced connections. The connections, shear pockets and haunches were cast with one continuous placement on an afternoon in early May with temperatures in the mid-60's °F and 50-60% relative humidity (Table 20). The panels were then tested one week later in a controlled environment. The grout remained in the laboratory conditions; low humidity and temperatures between 60-70°F. Throughout the tests, no shrinkage cracks were observed in the shear pockets. The grouts were observed from the day of their casting through the end of the testing, or approximately 42 days. The performance was considered satisfactory.



Figure 65. Pocket Layout on the Test Panels

The second test specimen was built after the first in the same laboratory with the same type of grout. The procedures were exactly the same. The block-outs had been formed against a smooth piece of plywood in the precast plant and were therefore extremely smooth. The block-outs were prepared by wetting them down to a moist surface condition prior to grouting. The only difference in this placement was the grout was placed in the shear pockets and haunches at the same time. The casting was done at the end of July with high temperature around 70°F and 100% humidity. The specimens were cast indoors, but there were thunderstorms all afternoon, and the overhead garage doors were open most of the time, resulting in high indoor humidity (Table 20).

Table 20. Average Weather Conditions When Grouting the Shear Pockets

Panel Test	Temperatures – Day of the Grout Pour	Humidity – Day of the Grout Pour
Reinforced Connections	64 Degrees Inside/Outside	50-60% Humidity
Post-tensioned 1 167 psi	70 Degrees Outside/Inside	100% Humidity – Thunderstorms
Post-tensioned 2 340 psi	70 Inside, Low 60's Outside	100% Humidity – Rainy Day

The grouts in the second specimen began to shrink right after placement. In this specimen, cracks appeared around the edge of half of the block-outs on the day after grouting. At the beginning and end of the load test, the average widths were measured using a crack card (0.005 in precision). Average widths were computed by taking the width measurements around the entire perimeter of the block-out. The average crack widths of each pocket are listed in Table 21. A typical crack pattern is shown in Figure 66. The number of cycles undergone was written next to the crack as it became visible in the test. Cracks were observed in every pocket, nearly without exception, between the panels and grout in the second test. The extensive cracking warranted further investigation.

Table 21. Average Crack Widths in the Shear Pockets of the Second Specimen

Pocket Number	Initial Average Width (14 Days) (in)	Final Average Width (53 Days) (in)
1	0.010	0.010
2	0.015	0.020
3	0.020	0.020
4	0.015	0.015
5	0.015	0.020
6	0.015	0.015
7	0.005	0.005
8	0.010	0.010
9	0.015	0.020
10	0.020	0.025
11	0.010	0.010
12	0.005	0.005
Average	0.015	0.015



Figure 66. Typical Shrinkage Crack Patterns in the Shear Pockets Prior to Loading

Grout Testing in the Shear Pockets on the Third Transverse Connection Specimen

On the third test specimen, new bonding techniques between the concrete panels and the grouts in the pockets were investigated. Six different types of joining methods were used. The first method was a control specimen built with the original smooth, moistened concrete. The second method had a roughened surface. It was constructed by placing a retarder on the pocket surface prior to casting at the precast plant. The paste was then sprayed off with water when removing the forms approximately 18 hours later. The third method employed sandblasting the surface of the pocket after removing the formwork at the precast plant. The fourth method was to apply a concrete bonding agent (vinyl acetate emulsion) to the pocket approximately thirty minutes (per the manufacturer's recommendation) prior to placing the grout to bond the surfaces. The fifth method was to place a water stop (see Figure 23f) in the panel during casting that fit across the interface between the concrete and grout. The sixth and last method was to place a grout paste on the surface of the pocket approximately one hour before placing the grout.

Crack widths were measured once a week from the day of the first test until the conclusion of the cyclical loading. Observations were made from February 5, 2008, to April 19, 2008, or over 74 days.

Table 22 shows the final crack widths for the third specimen. The first post-tensioned pockets were all built the same way as the control pockets in the second post-tensioned test. The averages are reported to the nearest 0.005 in, which was the precision of the crack gage.

Almost every method used to reduce cracking resulted in smaller crack widths than the control pockets in this specimen (0.010 in) and the pockets in the second specimen (Table 21, average crack width 0.015 in). The control and epoxy-coated pockets consistently had the largest cracks among all of the tests. The water-stop and sandblasted pockets consistently performed well. The exposed-aggregate and grouted pockets also exhibited small crack sizes.

Table 22. Average Crack Widths in the Grout Pockets in the Third Specimen

Shear Stud Pocket Surface Treatment	Final Average Width, in
1 – Sandblasted	0.005
2 – Exposed Aggregate	0.005
3 – Control	0.010
4 – Control	0.010
5 – Epoxy	0.005
6 – Epoxy	0.010
7 – Sandblasted	0.000
8 – Exposed Aggregate	0.000
9 – Water-Stop	0.005
10 – Water-Stop	0.000
11 – Grout	0.005
12 – Grout	0.000
Average	0.005

A ponding test was performed on the shear pockets during the cyclical testing. This was accomplished with the same procedure used in the ponding tests for the transverse connections. At set intervals, the surface was covered with water for two hours. The bottom outer edges of the pockets were monitored for leaks. The pockets did not have a clearly identifiable interface on the bottom of the panels because they intersected the haunch (Figure 67). In these tests, the haunch forming material was removed so that any water that filtered through the pocket and the haunch could be observed. Table 23 shows qualitative results observed during the tests.

Table 23. Ponding Results – Leaks Through the Shear Pockets

Cycles	Control	Grouted Surface	Water Stops	Epoxy	Exposed Aggregate	Sand-Blasted
0	None	None	None	None	None	None
1	None	1 Complete Leak	None	None	None	None
10000	None	1 Complete Leak	None	None	None	None
50000	2 Partial Leaks	1 Complete, 1 Partial	None	None	1 Partial Leak	None
100000	2 Partial Leaks	1 Complete	None	None	2 Partial Leaks	None
500000	2 Partial Leaks	1 Complete, 1 Partial	None	None	1 Partial Leak	1 Very Slight
1000000	1 Partial Leak	2 Complete	1 Slight Vertical Leak	2 Slight	1 Partial Leak	1 Slight

The pockets that leaked the least were the epoxy-primed pockets, the pockets with water-stops, and the sandblasted pockets. The exposed-aggregate detail was satisfactory but the control and grouted-surface detail both performed poorly (Figure 67). The control pockets consistently leaked the most. One of the grouted-surface pockets had a small imperfection that caused the leaking to appear severe; however, the other grouted-surface pocket also leaked considerably. The one leak in the water-stop pocket was in a vertical crack that appeared to extend beyond the width of the water-stop in the center of the pocket.



Figure 67. Complete Leaking in the Haunch Beneath a Shear Pocket

CONCLUSIONS

Transverse Connection Tests

Construction

The general construction processes were similar to methods from previous research or traditional deck construction. Some of the specific forming methods, materials, and procedures did deviate. The following conclusions were drawn from the construction of the transverse connection specimens.

- The panels were easy to build in the precast plant; however, the addition of suspended parts or complex geometry slowed the process. In particular, the HSS sections, the water-stops, the anchor bolt assembly, and the post-tensioned anchors took more time to install.
- Fiberboard formwork for the haunches contained the grout, was easy to adjust, and was stiff enough to withstand the weight of the deck panels.
- The looped bar connections and post-tensioned connections had sufficient tolerance and were quick to install. The drop-in bar connection did not have sufficient tolerance to align the rebar and was difficult to setup.
- Using threaded rods to hold up the wooden formwork created weak points in the grouted connections. Tying the formwork to the reinforcing bars prevented weak points in the top surface of the deck slab.
- Adding pea gravel to the grout for the connections did not take additional time, but workability suffered and segregation occurred when the mix was not placed within 15 minutes.
- Having a sufficiently large workforce was essential at all stages because of the time-dependent nature of installing the panels. This was particularly true when setting the panels, placing the grout, and post-tensioning the deck panels.

Performance

The transverse connections in the deck panels were exposed to 1,000,000 cycles to simulate truck loads. This value corresponded to 50 years of service for the subject rural bridge in Virginia. The transverse connection tests were based on the expected loading conditions of the Virginia bridge. A number of observations were made for the best connection to use on this bridge.

- The concrete-to-grout interface is the weakest point in all of the connections. The tensile strength of the interface is weaker than the cohesive tensile strengths of the concrete and grouts tested.
- Shrinkage cracking will occur at the concrete-to-grout interface if no surface preparation technique is used, regardless of the reinforcement configuration of the connection.
- Imperfections due to tie rods or formwork will cause cracking in the grouts.
- Reinforced connections under tensile forces will crack under HS-20 loading, primarily between the concrete and grout. Cracking occurs immediately upon loading.
- In the post-tensioned transverse connections, cracking was first observed at a net stress level of 125 psi (the load-induced stress minus the pre-compression). This corresponds to a tensile strength of $1.9\sqrt{f'_c}$ in the transverse connection, where the specified strength, f'_c , is the weaker of the compressive strengths of the grout in the connection and concrete in the panels.
- A post-tensioning level of 340 psi effective stress prevented significant cracking in the top surface of the connection and resulted in linear strain behavior at the transverse connection.
- A post-tensioning level of 167 psi resulted in significant cracking in the top surface of the connection and a non-linear strain response at the transverse connection.
- The drop-in bar connection cracked significantly. The concrete adjacent to the transverse connection exhibited almost no strain after cracking.
- The looped reinforcing bar connection had minor cracks at both grout-to-concrete interfaces. At the transverse connection, the concrete carried a small amount of strain.
- For this bridge, an effective prestress level of 340 psi kept crack widths below 0.005 in, which prevented any leaks from occurring in the transverse connections.
- The neutral axis, based on the strain measurements, remained constant for the post-tensioned connection with initial prestress of 340 psi.
- The reinforced connections and 167-psi post-tensioned connections had neutral axes that moved downward toward the neutral axis of the beam, away from the deck, during cyclical loading.
- The surface strain under the maximum service load remained constant for the 340-psi connection. The drop-in bar connections experienced the largest increase in surface strain during the tests, followed closely by the 167-psi connections. The looped bar connection had consistent surface strains.

Design

The following conclusions about future designs can be drawn from the testing program:

- The post-tensioned connection with initial stress of 340 psi in the connection performed the best based on cracking, deformation, ponding, and strain distribution measurements and is should perform very well for future transverse connections.
- Based on comparisons with more detailed finite element models, the simple sectional model developed by Bowers (2007) is acceptable for determining time dependent stress redistributions.
- A maximum tensile stress at the grout-to-concrete interface at the connection of $3.0\sqrt{f'_c}$. (where f'_c is the weaker of the concrete and grout compressive strengths) should eliminate, or greatly reduce, cracking and this stress level is consistent with the maximum tensile stress allowed by AASHTO in aggressive environments (AASHTO, 2012).
- The looped reinforcing bar connection had minor cracking and the second smallest leaks during testing. If post-tensioning is not an option, then the looped reinforcing bar connection should provide satisfactory performance.
- The top surface of looped bar connections should be covered with an impermeable barrier to increase its lifespan and reduce effects from leaks.
- Looped bar connections should only be used on low volume roads.
- The 167-psi connections and drop-in bar connections did not perform well based on observed leaking, extensive cracking and large deformations.
- The 167-psi connections and drop-in bar connections are not expected to perform well for full-depth deck panels on bridges that are continuous over multiple spans.

RECOMMENDATIONS

1. *VDOT's Structure and Bridge Division should design prestressed full-depth deck panel-to-panel connections using post-tensioning whenever possible, particularly for bridge decks on continuous bridges. The net tension across the connection after all losses and under full live load should be no greater than $3.0\sqrt{f'_c}$, where f'_c is the lower of the concrete and grout compressive strengths.*
2. *VDOT's Structure and Bridge Division should use the looped reinforcing bar detail when post-tensioning is not feasible. The non-prestressed connection should perform adequately on simply supported structures, but an overlay is recommended to reduce water leakage onto the superstructure elements below the deck. This detail should not be used on continuous bridges with high truck traffic.*
3. *VDOT's Structure and Bridge Division should specify that the surface of the block-out pockets should either be sandblasted and saturated surface dry or have an epoxy bonding agent applied immediately prior to grouting operations. These two surface preparations should reduce cracking at the interface. An overlay will also help reduce leaking.*

BENEFITS AND IMPLEMENTATION

The two primary benefits of using full-depth, precast concrete bridge deck panels are rapid construction and high-quality concrete. The primary challenge is designing the panel-to-panel and panel-to-beam connections to be durable over the long term and not result in system stiffness degradation. Precast bridge deck panel systems built in accordance with the recommendations in this report should prove to be long lasting and low maintenance. The recommendations were implemented for a bridge in southwestern Virginia that carries Route 65 over Staunton Creek. A subsequent study of the construction process, the behavior under live load, and the time-dependent behavior (Woerheide, 2012) over the first 6 months of service showed the system to work as expected and will be documented in a separate report.

The recommendations in this report will be implemented by the State Structure and Bridge Engineer by incorporating these recommendations into the *Manual of the Structure and Bridge Division, Part 2 – Design Aids* during the revisions in spring 2016. Any future projects using full-depth precast deck panels will require the modified details and procedures.

ACKNOWLEDGMENTS

This project was sponsored by the Federal Highway Administration and the Virginia Center for Transportation Innovation and Research (VCTIR). The authors gratefully acknowledge the guidance provided by the engineers at VCTIR and VDOT, including Michael Brown, Bernie Kassner, Teresa Gothard, Chris Blevins, and Garry Lovins. The opinions expressed in this report are those of the authors and not necessarily those of the sponsors.

REFERENCES

- AASHTO. (1996). *Standard Specifications for Highway Bridges*. American Association of State Highway and Transportation Officials, Washington, DC.
- AASHTO. (2012). *AASHTO LRFD Bridge Design Specifications*. American Association of State Highway and Transportation Officials, Washington, DC.
- ACI Committee 224. (2008). Control of Cracking in Concrete Structures. ACI 224R-01 (Reapproved 2008). American Concrete Institute, Farmington Hills, MI.
- ACI Committee 318. (2008). *Building Code Requirements for Structural Concrete and Commentary*. ACI 318-08. American Concrete Institute, Farmington Hills, MI.
- Badie, S.S., and Tadros, M.K. (2008). *Full-Depth Precast Concrete Bridge Deck Panel Systems*. NCHRP Report 584. Transportation Research Board of the National Academies, Washington, DC.

- Bowers, S. (2007). *Recommendations for Longitudinal Post-Tensioning in Full-Depth Precast Concrete Bridge Deck Panels*. M.S. Thesis, Virginia Tech, Blacksburg.
- BS EN 1992-1-1 (2004). Eurocode 2: Design of Concrete Structures – Part 1-1: General Rules and Rules for Buildings, British Standards Institution, London.
- Holguin, J. (2005). Gridlock Driving Up Wasted Time. CBS News. <http://www.cbsnews.com/news/gridlock-driving-up-wasted-time/>. Accessed April 4, 2014.
- French, C., Eppers, L., Le, Q., and Hajjar, J. (2007). Transverse Cracking in Concrete Bridge Decks, Transportation Research Record 1688, Jan. 2007, pp. 21-29.
- Issa, M.A., Idriss, A.-T., Kaspar, I.I., and Khayat, S.Y. (1995). Full Depth Precast and Precast, Prestressed Concrete Bridge Deck Panels. *PCI Journal*, Vol. 40, No. 1, pp. 59-80.
- Krauss, P.D., and Rogalla, E.A. (1996). Transverse Cracking in Newly Constructed Bridge Decks. NCHRP Report 380. Transportation Research Board of the National Academies, Washington, DC.
- Longman, P.J. (2001). “American Gridlock”, US News and World Report, V. 130, No. 21, May 28, 2001, pp. 16-22.
- New England Region of PCI. (2002). *Design Guidelines for Full Depth Precast Concrete Deck Slabs*. PCINER-02-FDPCDS. Prestressed/Precast Concrete Institute, Chicago.
- Scholz, D.P., Wallenfelsz, J.A., Lijeron, C., and Roberts-Wollmann, C.L. (2007). Recommendations for the Connection Between Full-Depth Precast Bridge Deck Panel Systems and Precast I-Beams. VTRC 07-CR17. Virginia Transportation Research Council, Charlottesville.
- Sullivan, S., and Roberts-Wollmann, C.L. (2008). Experimental and Analytical Investigation of Full-Depth Precast Deck Panels on Prestressed I-Beams. VTRC 09-CR4. Virginia Transportation Research Council, Charlottesville.
- Swartz, B.D., and Schokkera, A. (2008). Design Guide Development for Post-Tensioned Bridge Decks. *PTI Journal*, Vol. 6, No. 2, pp. 7-20.
- Swenty, M.K. (2009). *The Investigation of Transverse Joints and Grouts on Full Depth Concrete Bridge Deck Panels*. Ph.D. Dissertation, Virginia Tech, Blacksburg.
- Woerheide, D. (2012). *Structural Performance of Longitudinally Post-Tensioned Precast Deck Panel Bridges*. M.S. Thesis, Virginia Tech, Blacksburg.